# Highly Reflective Foveal Region in Optical Coherence Tomography in Eyes with Vitreomacular Traction or Epiretinal Membrane

*Kazushige Tsunoda, MD,[1] Ken Watanabe, MD,[2] Kunihiko Akiyama, MD,[2] Tomoaki Usui, MD,[3] Toru Noda, MD[2]*

***Objective:*** To report the optical coherence tomography (OCT) findings in eyes with vitreomacular traction (VMT) or with an epiretinal membrane (ERM).

***Design:*** Retrospective case series.

***Participants:*** Fifty-four eyes of 45 consecutive patients with subjective visual disturbances resulting from VMT or idiopathic ERM were studied.

***Methods:*** The morphologic features of the photoreceptor layer at the foveal center were determined and the central foveal thickness (CFT) was measured by spectral-domain (SD) OCT.

***Main Outcome Measures:*** The morphologic characteristics of the foveal region observed by SD OCT.

***Results:*** A roundish or diffuse highly reflective region was observed between the photoreceptor inner segment/outer segment junction line and the cone outer segment tip line at the center of the fovea. This highly reflective region was present in 7 of 7 cases of VMT and 30 of 47 cases of ERM. In the ERM cases, the mean CFT of the cases with the highly reflective region was significantly thicker than that in cases without it. The highly reflective region disappeared when the inward traction on the fovea was released surgically or spontaneously.

***Conclusions:*** The highly reflective region is a characteristic sign observed in the OCT images of eyes with VMT and ERM, and it has been termed the *cotton ball sign* after its appearance. The presence of the cotton ball sign indicates an inward traction on the fovea and may be a predictor of visual impairment.

***Financial Disclosure(s):*** The author(s) have no proprietary or commercial interest in any materials discussed in this article. *Ophthalmology 2012;119:581–587 © 2012 by the American Academy of Ophthalmology.*

Vitreomacular tractions (VMTs) and epiretinal membranes (ERMs) cause morphologic distortions of the retinal surface and lead to functional changes such as metamorphopsia and decreased visual acuity.[1–4] Surgical removal of the VMT or ERM is effective in restoring good visual function. Similar recovery is obtained when the traction is released spontaneously.

Optical coherence tomography (OCT) has shown that a vertical or tangential traction of the retina causes wrinkling of the internal limiting membrane, flattening of the foveal pit, and intraretinal cystic changes.[5–11] Moreover, recent spectral-domain (SD) OCT has shown that eyes with VMT and ERM have structural abnormalities of the photoreceptors at the fovea, for example, loss of the photoreceptor inner/outer segment (IS/OS) junction line.[12–17] The abnormalities in the IS/OS junction line were correlated significantly with poorer visual function; however, the relationship between these abnormal OCT findings and the foveal traction has not been determined definitively. The SD OCT studies have shown a roundish or diffuse highly reflective region at the center of the fovea in all of the cases of VMT and in cases of ERM with increased central foveal thickness (CFT). The authors named this highly reflective region the *cotton ball sign*, after its appearance.

The aim of this study was to determine the characteristics and correlations of this abnormal sign in the OCT images and the retinal physiologic features. This study showed that the cotton ball sign disappeared when the foveal traction was released surgically or spontaneously. The presence of the cotton ball sign is good evidence that there is inward traction on the photoreceptors.

## Patients and Methods

This was a retrospective case series performed in the Department of Ophthalmology, National Tokyo Medical Center, Tokyo, Japan. Informed consent was obtained from all of the subjects for the tests after an explanation of the procedures to be used. The procedures used adhered to the tenets of the Declaration of Helsinki, and approval to perform this study was obtained from the Review Board/Ethics Committee of the National Tokyo Medical Center.



ISSN 0161-6420/12/$–see front matter
doi:10.1016/j.ophtha.2011.08.026

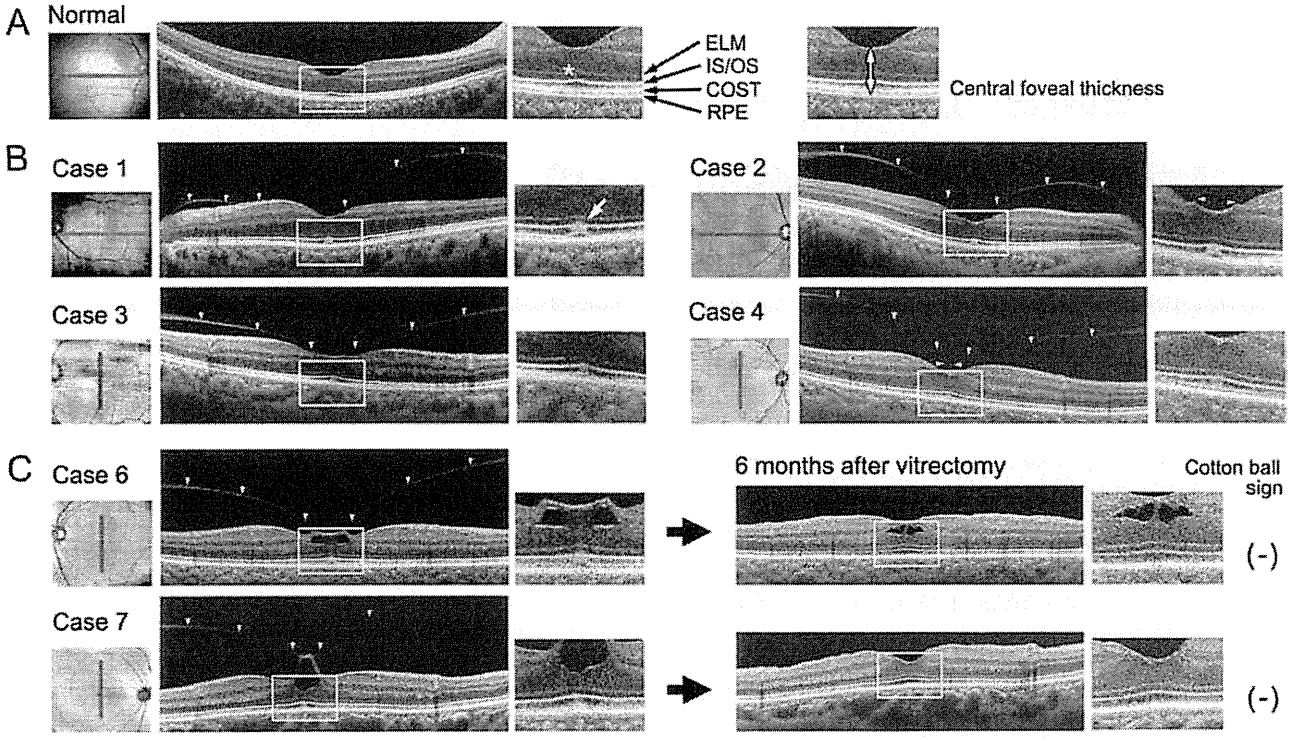


Figure 1. Optical coherence tomography (OCT) images of eyes with vitreomacular traction (VMT) with the foveal images magnified on the right. Fundus images on the left indicate the location of the OCT scans. A, Normal control OCT image from a 22-year-old woman. Outer retinal structures with high reflectivity are indicated by arrows: external limiting membrane (ELM), photoreceptor inner segment/outer segment (IS/OS) junction, cone outer segment tip (COST) line, and retinal pigment epithelium (RPE). The foveal bulge is indicated by an *asterisk*. The central foveal thickness is measured as the distance between the inner retinal surface and inner border of the RPE (*white arrow*). B, Optical coherence tomography images of eyes with VMT. The border of the posterior vitreous is indicated by *arrowheads*. The roundish highly reflective region between IS/OS junction line and COST line is the cotton ball sign and is identified by a *white arrow* in case 1. C, Two eyes with VMT before and 6 months after vitrectomy. In both cases, the vitreous traction was released and the cotton ball sign was not present after the surgery.

## Inclusion and Exclusion Criteria

Fifty-four eyes of 45 patients (average age, 69.0±9.2 years; range, 34–85 years) with subjective visual disturbances resulting from VMT or idiopathic ERM were studied. The patients were examined between October 2009 and January 2011; 7 eyes had VMT and 47 eyes had ERM (Table 1, available at http://aaojournal.org). A VMT was defined as a vitreomacular adhesion at the foveal region without an apparent ERM over the entire macular region. All of the cases with VMT were focal VMT, according to the definition of Koizumi et al.[11] The exclusion criteria were: (1) eyes with a history of retinal inflammatory or vascular diseases, such as branch vein occlusion, uveitis, and retinal detachment; (2) eyes with advanced lens opacification or any other ocular diseases that could cause visual disturbances; (3) eyes with strong vitreal traction on the retina that led to either lamellar or pseudomacular holes; (4) eyes in which the center of the fovea could not be determined in the OCT images because of a lack of a bulge-like structure of the IS/OS junction line at the fovea[18]; and (5) cases whose OCT image did not have enough signal intensity for evaluation, that is, average intensity of the OCT signal less than 8/10.

All patients underwent a complete ophthalmologic examination, including best-corrected visual acuity using a Landolt C chart, biomicroscopy of the fundus, fundus photography, and OCT.

## Optical Coherence Tomography

The OCT images were obtained with SD OCT (Cirrus HD-OCT, versions 4.5 and 5.1; Carl Zeiss Meditec, Dublin, CA). After dilatation of the pupil, patients were asked to fixate on a target, and 5-line scans with 4 averages were performed both horizontally (length, 9.0 mm) and vertically (length, 6.0 mm). The distance between each scan line was set to be 0.075 mm, or, in some cases, 0.025 mm, to determine the location of foveal bulge. The foveal bulge is a dome-shaped structure of the IS/OS junction line corresponding to the foveal center (Fig 1A, asterisk). If the foveal bulge could not be obtained by the point of fixation, the location of the scan line was shifted and the OCT images were taken repeatedly until the foveal bulge was present in the image.

The CFT was defined as the distance between inner retinal surface and inner border of retinal pigment epithelium (RPE; Fig 1A) and was measured with the built-in scale of the OCT system. The diameter of the highly reflective region was measured in one of the scanned profiles that showed the maximum diameter of the region. For patients who underwent vitrectomy, the OCT images were recorded 6 months after the surgery.

## Vitrectomy for Vitreomacular Traction and Epiretinal Membranes

Two of 7 eyes with VMT and 18 of 47 eyes with an ERM underwent 23- or 25-gauge 3-port vitrectomy by 2 experienced

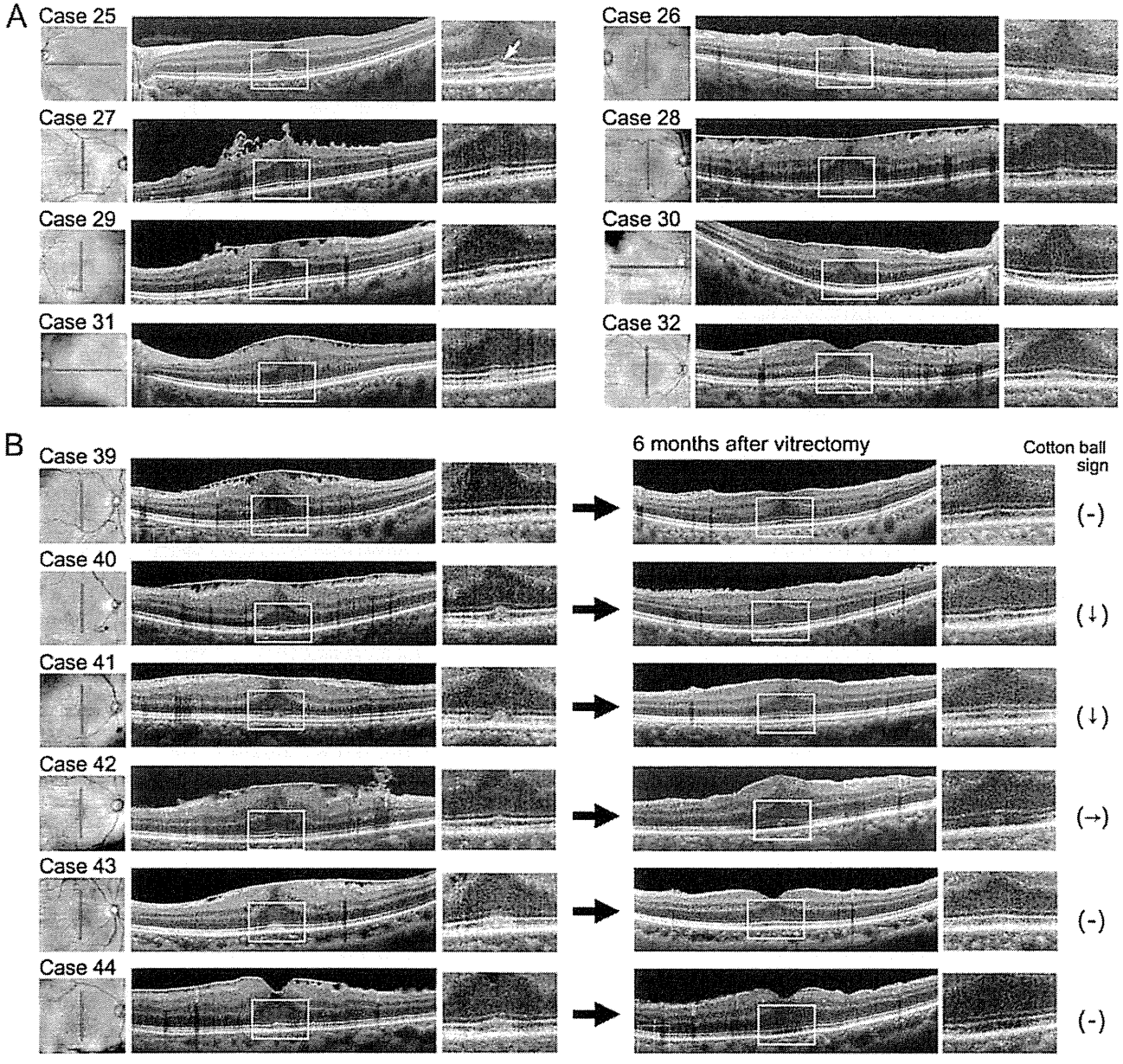


Figure 2. Optical coherence tomography (OCT) images of eyes with an epiretinal membrane (ERM) with the foveal area magnified (*right*). Fundus photographs (*left*) indicate the location of OCT scans. A, Optical coherence tomography images of eyes with an ERM. The roundish highly reflective region between inner segment/outer segment junction line and cone outer segment tip line is the cotton ball sign and is identified by a *white arrow* in case 25. B, Optical coherence tomography images of eyes with an ERM before and 6 months after vitrectomy. In cases 39, 43, and 44, the cotton ball sign disappeared after surgery. In cases 40 and 41, the cotton ball sign did not disappear, but became more indistinct after the surgery. In case 42, the cotton ball sign was still observed clearly after the surgery. The highly reflective region in cases 25, 40, and 41 appeared roundish, but that in cases 31, 43, and 44 appeared indistinct and diffuse.

surgeons (K.A. and K.W.). During the vitrectomy, a posterior hyaloid detachment was made, and the ERM was removed. The internal limiting membrane was peeled with forceps in all cases. Phacoemulsification with intraocular lens implantation was performed during the same surgery in 17 of the 20 eyes.

## Statistical Analysis

Student *t* tests were performed to compare the CFT with the presence of the highly reflective region in cases of ERM before and after surgery. Statistical analysis was performed using Microsoft Office Excel 2007 (Microsoft, Redmond, WA). *P* values $<0.05$ were taken as statistically significant.

## Results

The outer retinal structures detected in the OCT image of normal retinas consisted of (1) the external limiting membrane, (2) the IS/OS junction line, (3) the cone outer segment tip (COST) line,

Table 2. Cotton Ball Sign and Central Foveal Thickness

| | Cotton Ball Sign | Central Foveal Thickness (μm) | | P |
|---|---|---|---|---|
| | | *Mean* | *Standard Deviation* | |
| VMT (n = 7) | Observed | 252.0 | 87.1 | |
| ERM before surgery (n = 47) | Not observed (n = 17) | 289.3 | 96.0 | 0.0000076* |
| | Observed (n = 30) | 445.7 | 102.2 | |
| | Total (n = 47) | 389.1 | 124.7 | |
| ERM after surgery (n = 16) | Disappeared (n = 8) | 300.0 | 28.6 | 0.00033† |
| | Not disappeared (n = 8) | 423.3 | 59.0 | |

ERM = epiretinal membrane; VMT= vitreomacular traction.
*t test between ERM with and without cotton ball sign.
†t test between ERM with and without the disappearance of cotton ball sign after vitrectomy.

(4) the RPE, and (5) the foveal bulge, which is a dome-like structure of the external limiting membrane and IS/OS junction line caused by an elongation of the cone outer segments at the fovea (Fig 1A).[18–20]

A highly reflective region was present in all of the eyes with VMT (Table 1, available at http://aaojournal.org). The OCT images of 6 VMT cases without (Fig 1B) or with (Fig 1C) vitrectomy are shown with the foveal images magnified. In all the cases, a separation of the vitreous from the retina occurred except in the limited region around the center of the fovea (Fig 1A, B, arrowheads), and the foveal center was pulled toward the vitreous cavity. In case 1, a roundish, highly reflective region resembling a cotton ball can be seen between the IS/OS junction line and COST line at the center of the fovea. The COST line can be seen to be pulled inward just below the highly reflective region and is separated from the RPE (Fig 1B, case 1, white arrow). Similar findings were observed in cases 2 and 6. In all of the other cases (cases 3, 4, and 7), the highly reflective region was observed at the same location, but its borders were more indistinct than in cases 1, 2, and 6. Two of the eyes with VMT underwent vitrectomy, and the highly reflective region could not be observed in the OCT image obtained 6 months after the vitrectomy (Table 1, available at http://aaojournal.org; Fig. 1C).

The SD OCT examinations of the 47 eyes with an ERM showed that the highly reflective region was present in 30 eyes (63.8%; Table 1, available at http://aaojournal.org). The OCT images of 8 ERM cases without (Fig 2A) or with (Fig 2B) treatment are shown with the foveal images magnified. In all the cases, the epiretinal membrane covered the entire macular region, and the tangential traction elevated the retinal surface at the fovea, leading to a loss of the foveal pit. In case 25, the highly reflective region was observed between the IS/OS junction line and COST line at the center of the fovea (Fig 2A, case 25, white arrow). As in the eyes with VMT, the COST line was pulled inward just below the highly reflective region and was separated from the RPE. The highly reflective region was observed at the same location in all eyes. The regions appeared roundish in some cases (e.g., cases 25, 40, and 41) and indistinct and diffuse in other cases (e.g., cases 31, 43, and 44).

Vitrectomy was performed on 16 eyes with an ERM, and 6 months after surgery, the highly reflective region was not observed in 8 cases, became smaller and more indistinct in 2 cases, or could still be observed in 6 cases (Table 1, available at http://aaojournal.org; Fig 2B).

The diameter of the highly reflective region varied from 96 to 180 μm with a mean 130.4±36.4 μm in the eyes with a VMT and from 80 to 288 μm with a mean of 172.7±65.8 μm in eyes with an ERM. The highly reflective region was always present between the IS/OS junction and COST lines, except for case 41, where the IS/OS junction line was disrupted at the foveal center and the round, highly reflective region penetrated into the outer nuclear layer (Fig 2B).

The mean CFT was 252.0±87.1 μm in eyes with VMT and 389.1±124.7 μm in eyes with an ERM (Table 2). For the 47 eyes with an ERM, the mean CFT of the eyes with the highly reflective region was 445.7±102.2 μm, which was significantly thicker than that in eyes without the highly reflective region at 289±96.0 μm. For the 16 eyes with an ERM for which vitrectomy was performed, the CFT was measured 6 months after surgery. The mean CFT of the 8 eyes in which the highly reflective region did not disappear was 423.3±59.0 μm, which was significantly thicker than that in the 8 eyes in which the highly reflective region disappeared at 300.0±28.6 μm.

In one case (case 5) with a spontaneous vitreous detachment, there was a recovery of the microstructural damage of the photoreceptor layer in the OCT images. Case 5 was a 34-year-old woman who had a sudden decrease of her vision together with floaters in her right eye (Table 1, available at http://aaojournal.org; Fig 3). Her best-corrected visual acuity was 0.6 in the right eye and 1.2 in the left eye. She was referred to the authors' hospital 10 days after the onset of her symptoms, and fundus biomicroscopic examination showed that a thick posterior hyaloid membrane was detached from the posterior pole in her right eye. In the OCT image, there was a clear, highly reflective region, although the vitreomacular traction had been released (Fig 3A). Moreover, the photoreceptor IS/OS junction line seemed to be pulled inward at the foveal center, and there was a local defect of the COST line just beneath the highly reflective region (Fig 3A, white arrow). In the OCT image obtained 30 days after the onset, the highly reflective region was not present, and the photoreceptor structures, including the IS/OS junction and COST lines, appeared normal (Fig 3B, white arrow). The visual acuity also recovered to 1.0 at that time.

## Discussion

The SD OCT findings showed that all eyes (n = 7) with VMT and 63.8% of the eyes (30/47) with an ERM have a highly reflective region at the center of the fovea. This region can be roundish in some cases or diffuse and indistinct in other cases, and it was always located between the IS/OS junction and COST lines. This area was termed the *cotton ball sign* after its appearance. Related articles were searched for in PubMed with the following terms: *vitreomacular traction, epiretinal membrane*, and *optical coher-*

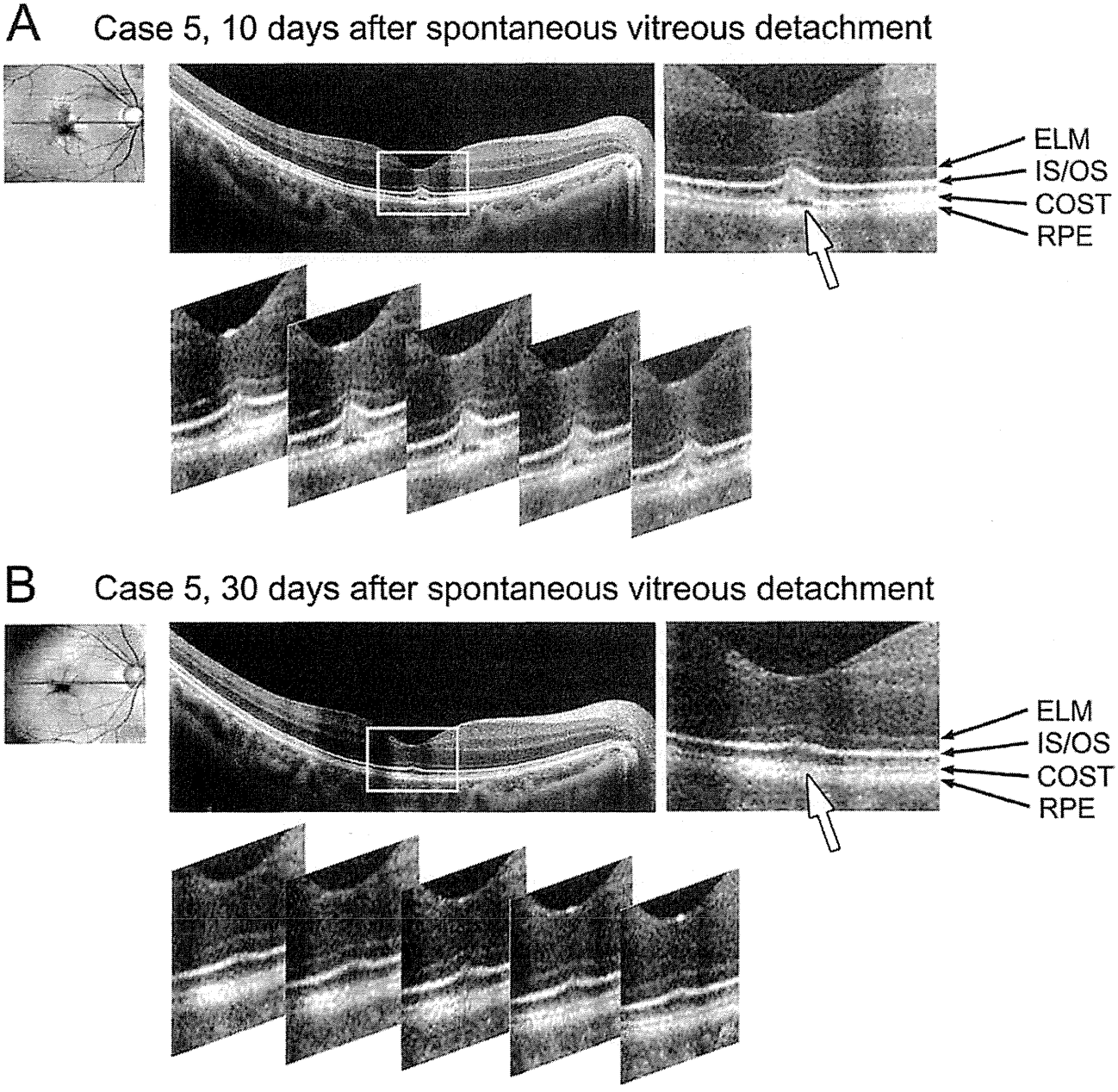


Figure 3. Optical coherence tomography (OCT) images of eyes with vitreomacular traction (case 5) in which a posterior vitreous detachment occurred spontaneously without surgery. Five horizontal OCT scans were obtained with an interscan distance of 20 μm. Five sequential profiles of the foveal region are aligned at the bottom, covering the central region of 80 μm of the fovea. A, Optical coherence tomography image obtained 10 days after spontaneous vitreous detachment. A round, highly reflective region (cotton ball sign) is present between the inner segment/outer segment (IS/OS) junction and cone outer segment tip (COST) lines at the foveal center. The center of IS/OS junction line is pulled inward and appears protruded compared with that in a normal OCT image (Fig 1A). The COST line is disrupted just below the highly reflective region (*white arrow*). B, Optical coherence tomography image obtained 30 days after the spontaneous vitreous detachment. The cotton ball sign is not present. The protrusion of IS/OS junction line is not distinct, and the COST line is continuous over the entire foveal region (*white arrow*). ELM = external limiting membrane; RPE = retinal pigment epithelium.

*ence tomography*. These articles were read, and none of them describes the same feature.

Even with the improved OCT instruments with higher spatial resolution, the region easily can be missed if the scanned lines do not pass through the foveal center, the intensity of the OCT signal is not strong enough, or both. Three-dimensional volume scans do not have enough traverse resolution, so OCT should be made with multiple scans with the highest resolution available. The mean diameter of the highly reflective region varied from 96 to 180 μm with a mean of 130.4±36.4 μm in the eyes with VMT and from 80 to 288 μm with a mean of 172.7±65.8 μm in

eyes with an ERM. This means that the distance between each scan line should be set to less than 75 μm in the Cirrus HD-OCT. For example, the consecutive OCT images of case 5 were obtained with 5-line scans with a distance between the scans of 20 μm (Fig 3A, bottom). Moreover, because the fixation point is sometimes shifted upward in cases of longstanding ERM, the OCT scan should be repeated until the true center of the fovea is scanned.

The cotton ball sign in the OCT images seemed to be strongly correlated with the inward traction on the retina. In eyes with VMT, local adhesions between the vitreous and retinal surface causes strong and direct inward traction over the entire depth of the foveal pit.[13,16] However, an ERM causes a tangential shrinkage of the retinal surface, and this leads to an inward retinal displacement of the fovea, regardless of the existence of a posterior vitreous detachment. This continuous tension also affects the photoreceptor layer, leading to mechanical damage of the photoreceptors and deterioration of visual function.[12,14,15] In this study, in eyes with VMT in which direct vitreous traction was present at the fovea, the cotton ball sign was always observed, although there was no apparent inward displacement of the fovea in cases 1 through 5 (Figs 1 and 3) and the CFT was normal, except in cases 6 and 7 (Table 1, available at http://aaojournal.org). In the eyes with an ERM, the mean CFT of the cases with the cotton ball sign was significantly thicker than that in eyes without the cotton ball sign (Table 2). These findings indicate that the continuous inward traction by the ERM was the cause of the cotton ball sign. In 8 of 16 cases that underwent vitrectomy, the cotton ball sign disappeared within 6 months and the CFT was significantly thinner than that in eyes where the cotton ball sign did not disappear. This indicated that disappearance of the highly reflective region was not the result of the removal of the ERM, but was most likely the result of the release of inward traction. It is notable that in cases where the cotton ball sign disappeared after surgery, the foveal pit reappeared because of release of inward traction (Fig 2B, cases 39, 43, and 44). However, in cases where the cotton ball sign did not disappear, the foveal area was still flat or even convex (Fig 2B, cases 40, 41, and 42). These highly reflective regions were observed only at the foveal center, even in cases where the entire macular region was thickened because of the ERM. There are 2 possible reasons for why the cotton ball sign is observed only at the foveal center in the ERM eyes. First, in cases in which the internal limiting membrane became flat because of the tangential traction by the ERM, the inward traction could be applied most strongly to the photoreceptors at the foveal center because of the presence of the foveal pit. Second, the cone photoreceptors at the fovea have an elongated shape and their diameter is much smaller than those at the parafoveal region. This characteristic anatomic structure makes them more susceptible to the minute structural changes that may lead to the increased reflectivity in the OCT.

An ERM usually is associated with macular edema and reduced reflectivity resulting from fluid accumulation; however, an increase in the reflectivity is observed rarely. Then the question arises on why the inward traction affected the reflectivity of the foveal center in the OCT images? The highly reflective region was always located between the IS/OS junction and COST lines. This region corresponds to the outer segment of cone photoreceptors, whose reflectivity is usually low. The photoreceptor outer segments (OSs) contain stacks of membranous discs that are rich in visual pigments, and the OSs are aligned parallel to the light pathway. The authors suggest that the inward traction on the retina changes the alignment of the OSs, which then increases their reflectivity. Directional reflectivity is known to exist in the retinal nerve fiber layer[21,22] and Henle's fiber layer.[23] Recently, Lujan et al[23] successfully distinguished Henle's fiber layer from the true outer nuclear layer by varying the angular incidence of the OCT beam on the retinal plane. The photoreceptor OSs are long cylindrical structures whose reflectivity may depend on the angular incidence of the OCT beam.

The second hypothesis for the highly reflective region is that the continuous inward traction causes microstructural damages to the cone OSs, leading to glial migration, glial scar formation, and photoreceptor degeneration.[24] However, it is not likely that these changes could be reversible and, particularly in case 5, would completely recover within 30 days after the release of mechanical traction (Fig 3, case 5).

The exact mechanism causing the highly reflective region was not determined, but there is very little possibility that this highly reflectivity region is an optical artifact, because it appeared when inward traction was forced to the outer retina, regardless of the existence of an ERM, and disappeared when the traction was released.

The cotton ball sign was present, despite good vision in the patients; 4 of 7 eyes with VMT and 9 of 30 eyes with an ERM with the cotton ball sign had best-corrected visual acuity of 0.8 or better (Table 1, available at http://aaojournal.org). This means that the cotton ball sign does not necessarily indicate a decrease in visual acuity, and it may be used as a predictor of visual impairment that would arise after longstanding inward traction at the fovea. Continuous foveal traction is known to cause microstructural damages in the photoreceptor layer,[12–16] and early detection of this sign may help in the management of these patients in preserving good vision.

## References


1. Jaffe NS. Vitreous traction at the posterior pole of the fundus due to alterations in the vitreous posterior. Trans Am Acad Ophthalmol Otolaryngol 1967;71:642–52.
2. Wise GN. Relationship of idiopathic preretinal macular fibrosis to posterior vitreous detachment. Am J Ophthalmol 1975; 79:358–62.
3. Smiddy WE, Maguire AM, Green WR, et al. Idiopathic epiretinal membranes: ultrastructural characteristics and clinicopathologic correlation. Ophthalmology 1989;96:811–20; discussion 821.
4. Gandorfer A, Rohleder M, Kampik A. Epiretinal pathology of vitreomacular traction syndrome. Br J Ophthalmol 2002;86: 902–9.
5. Puliafito CA, Hee MR, Lin CP, et al. Imaging of macular diseases with optical coherence tomography. Ophthalmology 1995;102:217–29.

6. Wilkins JR, Puliafito CA, Hee MR, et al. Characterization of epiretinal membranes using optical coherence tomography. Ophthalmology 1996;103:2142–51.
7. Meyer CH, Rodrigues EB, Mennel S, et al. Spontaneous separation of epiretinal membrane in young subjects: personal observations and review of the literature. Graefes Arch Clin Exp Ophthalmol 2004;242:977–85.
8. Johnson MW. Tractional cystoid macular edema: a subtle variant of the vitreomacular traction syndrome. Am J Ophthalmol 2005;140:184–92.
9. Schmidt-Erfurth U, Leitgeb RA, Michels S, et al. Three-dimensional ultrahigh-resolution optical coherence tomography of macular diseases. Invest Ophthalmol Vis Sci 2005;46: 3393–402.
10. Legarreta JE, Gregori G, Knighton RW, et al. Three-dimensional spectral-domain optical coherence tomography images of the retina in the presence of epiretinal membranes. Am J Ophthalmol 2008;145:1023–30.
11. Koizumi H, Spaide RF, Fisher YL, et al. Three-dimensional evaluation of vitreomacular traction and epiretinal membrane using spectral-domain optical coherence tomography. Am J Ophthalmol 2008;145:509–17.
12. Michalewski J, Michalewska Z, Cisiecki S, Nawrocki J. Morphologically functional correlations of macular pathology connected with epiretinal membrane formation in spectral optical coherence tomography (SOCT). Graefes Arch Clin Exp Ophthalmol 2007;245:1623–31.
13. Gaudric A. Macular cysts, holes and cavitations: 2006 Jules Gonin lecture of the Retina Research Foundation. Graefes Arch Clin Exp Ophthalmol 2008;246:1071–9.
14. Suh MH, Seo JM, Park KH, Yu HG. Associations between macular findings by optical coherence tomography and visual outcomes after epiretinal membrane removal. Am J Ophthalmol 2009;147:473–80.
15. Falkner-Radler CI, Glittenberg C, Hagen S, et al. Spectral-domain optical coherence tomography for monitoring epiretinal membrane surgery. Ophthalmology 2010;117:798–805.
16. Takahashi A, Nagaoka T, Ishiko S, et al. Foveal anatomic changes in a progressing stage 1 macular hole documented by spectral-domain optical coherence tomography. Ophthalmology 2010;117:806–10.
17. Odrobina D, Michalewska Z, Michalewski J, et al. Long-term evaluation of vitreomacular traction disorder in spectral-domain optical coherence tomography. Retina 2011;31:324–31.
18. Tsunoda K, Fujinami K, Miyake Y. Selective abnormality of cone outer segment tip line in acute zonal occult outer retinopathy as observed by spectral domain optical coherence tomography. Arch Ophthalmol 2011;129:1099–101.
19. Srinivasan VJ, Monson BK, Wojtkowski M, et al. Characterization of outer retinal morphology with high-speed, ultra-high-resolution optical coherence tomography. Invest Ophthalmol Vis Sci 2008;49:1571–9.
20. Fernandez EJ, Hermann B, Povazay B, et al. Ultrahigh resolution optical coherence tomography and pancorrection for cellular imaging of the living human retina. Opt Express [serial online] 2008;16:11083–94. Available at: http://www.opticsinfobase.org/abstract.cfm?URI=oe-16-15-11083. Accessed August 9, 2011.
21. Knighton RW, Huang XR. Directional and spectral reflectance of the rat retinal nerve fiber layer. Invest Ophthalmol Vis Sci 1999;40:639–47.
22. Knighton RW, Qian C. An optical model of the human retinal nerve fiber layer: implications of directional reflectance for variability of clinical measurements. J Glaucoma 2000;9: 56–62.
23. Lujan B, Roorda A, Knighton RW, Carroll J. Revealing Henle's fiber layer using spectral domain optical coherence tomography. Invest Ophthalmol Vis Sci 2011;52:1486–92.
24. Schuman SG, Koreishi AF, Farsiu S, et al. Photoreceptor layer thinning over drusen in eyes with age-related macular degeneration imaged in vivo with spectral-domain optical coherence tomography. Ophthalmology 2009;116:488–96.

## Footnotes and Financial Disclosures

Originally received: March 17, 2011.
Final revision: June 20, 2011.
Accepted: August 11, 2011.
Available online: November 23, 2011. Manuscript no. 2011-444.

[1] Laboratory of Visual Physiology, National Institute of Sensory Organs, Tokyo, Japan.

[2] Department of Ophthalmology, National Tokyo Medical Center, Tokyo, Japan.

[3] Akiba Eye Clinic, Niigata, Japan.

Financial Disclosure(s):
The author(s) have no proprietary or commercial interest in any materials discussed in this article.

Supported in part by research grants from the Ministry of Health, Labor and Welfare, Tokyo, Japan; and the Japan Science and Technology Agency, Tokyo, Japan.

Correspondence:
Kazushige Tsunoda, Laboratory of Visual Physiology, National Institute of Sensory Organs, 2-5-1 Higashigaoka, Meguro-ku, Tokyo 152-8902, Japan.
E-mail: tsunodakazushige@kankakuki.go.jp.

lone for the study. Allergan, Inc has provided unrestricted funds to DRCR.net for its discretionary use.
Role of the Sponsor: The funding organization participated in oversight of the conduct of the study and review of the manuscript but not directly in the design of the study, the conduct of the study, data collection, data management, data analysis, interpretation of the data, or preparation of the manuscript. As per the DRCR.net Industry Collaboration Guidelines (http://www.drcr.net), DRCR.net had complete control over the design of the protocol, ownership of the data, and all editorial content of presentations and publications related to the protocol.


1. Diabetic Retinopathy Clinical Research Network. A randomized trial comparing intravitreal triamcinolone acetonide and focal/grid photocoagulation for diabetic macular edema. *Ophthalmology*. 2008;115(9):1447-1449, 1449, e1-e10.
2. Bakri SJ, Pulido JS, McCannel CA, Hodge DO, Diehl N, Hillemeier J. Immediate intraocular pressure changes following intravitreal injections of triamcinolone, pegaptanib, and bevacizumab. *Eye (Lond)*. 2009;23(1):181-185.
3. Benz MS, Albini TA, Holz ER, et al. Short-term course of intraocular pressure after intravitreal injection of triamcinolone acetonide. *Ophthalmology*. 2006; 113(7):1174-1178.
4. Jonas JB, Degenring RF, Kreissig I, Akkoyun I, Kamppeter BA. Intraocular pressure elevation after intravitreal triamcinolone acetonide injection. *Ophthalmology*. 2005;112(4):593-598.
5. Clark AF, Wordinger RJ. The role of steroids in outflow resistance. *Exp Eye Res*. 2009;88(4):752-759.
6. Clark AF, Morrison JC. Steroid-induced glaucoma. In: Morrison JC, Pollack IP, eds. *Glaucoma: Science and Practice*. New York, NY: Thieme; 2003.


## Selective Abnormality of Cone Outer Segment Tip Line in Acute Zonal Occult Outer Retinopathy as Observed by Spectral-Domain Optical Coherence Tomography

Optical coherence tomography (OCT) plays an important role in the diagnosis of retinal diseases with minimal ophthalmoscopic changes. For example, in eyes with acute zonal occult outer retinopathy (AZOOR),[1-3] an abnormality of the photoreceptor inner segment–outer segment (IS/OS) junction found by OCT was spatially correlated with the region of visual field defect. Recent high-resolution spectral-domain OCT images have shown a thin line between the IS/OS junction and the retinal pigment epithelium. This line has been identified as the cone OS tip (COST) line.[4] However, the pathophysiological interpretation of its appearance has not been established, and the diagnostic value of the COST line has yet to be determined.

We report 2 cases of AZOOR, both of which showed acute central scotoma with an enlarged blind spot. The ophthalmoscopic and angiographic changes were minimal, but electroretinography (ERG) revealed reduced responses in the affected regions. In both cases, the IS/OS junction on the OCT image was normal, but the COST line was not present or appeared indistinct in the region of visual field defect. Our findings suggest that the COST line may be an early indicator of cone photoreceptor dysfunction in eyes with minimal ophthalmoscopic abnormalities.

Report of Cases. Patient 1 (a 24-year-old woman) and patient 2 (a 28-year-old woman) both had sudden unilateral visual disturbances following photopsia. The visual acuities were 0.02 OD and 1.5 OS in patient 1 and 0.15 OD and 1.5 OS in patient 2. Goldmann kinetic perimetry revealed a blind spot enlargement and central scotoma in the right eye of both patients (**Figure 1** and **Figure 2**). The anterior segment and fundus were normal; however, fluorescein angiography showed a slightly mottled hyperfluorescence around the macula in the affected eye of both patients. The full-field scotopic ERGs were normal, but there were phase delays in the photopic 30-Hz ERGs in the affected eyes: 5.7 milliseconds in patient 1 and 8.0 milliseconds in patient 2. In addition, the amplitudes of the photopic b-waves were reduced in both patients. The focal macular ERGs (ER80; Kowa Co, Tokyo, Japan, and Mayo Co, Nagoya, Japan) in the central 15° were almost flat in the affected eye in both patients. Neither patient had systemic disorders such as viral infections or autoimmune diseases.

Spectral-domain OCT (Carl Zeiss Meditec, Dublin, California) showed the IS/OS junction clearly, even in the region of the scotoma. However, the COST line was not detected in patient 1 and appeared indistinct in patient 2 (Figure 1 andFigure 2). Moreover, the bulgelike structure of the IS/OS junction at the fovea (with the foveal bulge indicating a domelike appearance of the IS/OS junction due to an elongated cone OS at the fovea)[7] could not be observed in the affected eyes. The visual disturbances of these patients did not recover, and these abnormalities in the OCT images were observed at all examinations for 50 months in patient 1 and 18 months in patient 2 after the onset.

Comment. To our knowledge, this is the first report of AZOOR where the boundary of the IS/OS junction in the OCT images was well preserved but the COST line was absent or indistinct from the initial examination through the entire follow-up period. Earlier studies demonstrated that a loss or irregularity of the IS/OS junction observed by OCT corresponded well with the visual field defects even at the early stages of AZOOR,[2-3] and the abnormality in the IS/OS junction can improve following recovery of the scotoma. These findings have led to the hypothesis that photoreceptor OS dysfunction is the primary lesion in AZOOR.

The COST line corresponds to the junction between the photoreceptor tips and the apical processes of the retinal pigment epithelium, where photoreceptor OS disc membranes are continuously shed for renewal.[6] Thus, the appearance of the COST line may reflect the normal function of the photoreceptor OSs more closely than the IS/OS junction. In fact, in all of the AZOOR cases we have recently examined, the COST line was always absent in the region of IS/OS abnormalities, suggesting that the abnormality of the COST line may precede that of the IS/OS junction. In our 2 cases, the fundus appeared normal and the IS/OS junction was clearly observed in the region of the COST line abnormality for 50 and 18 months after the onset. The focal macular ERGs, however, were markedly reduced in the affected areas. In the OCT images, the cone photoreceptor dysfunction corresponding to the region of scotoma could be detected only by the abnormality of the COST line.

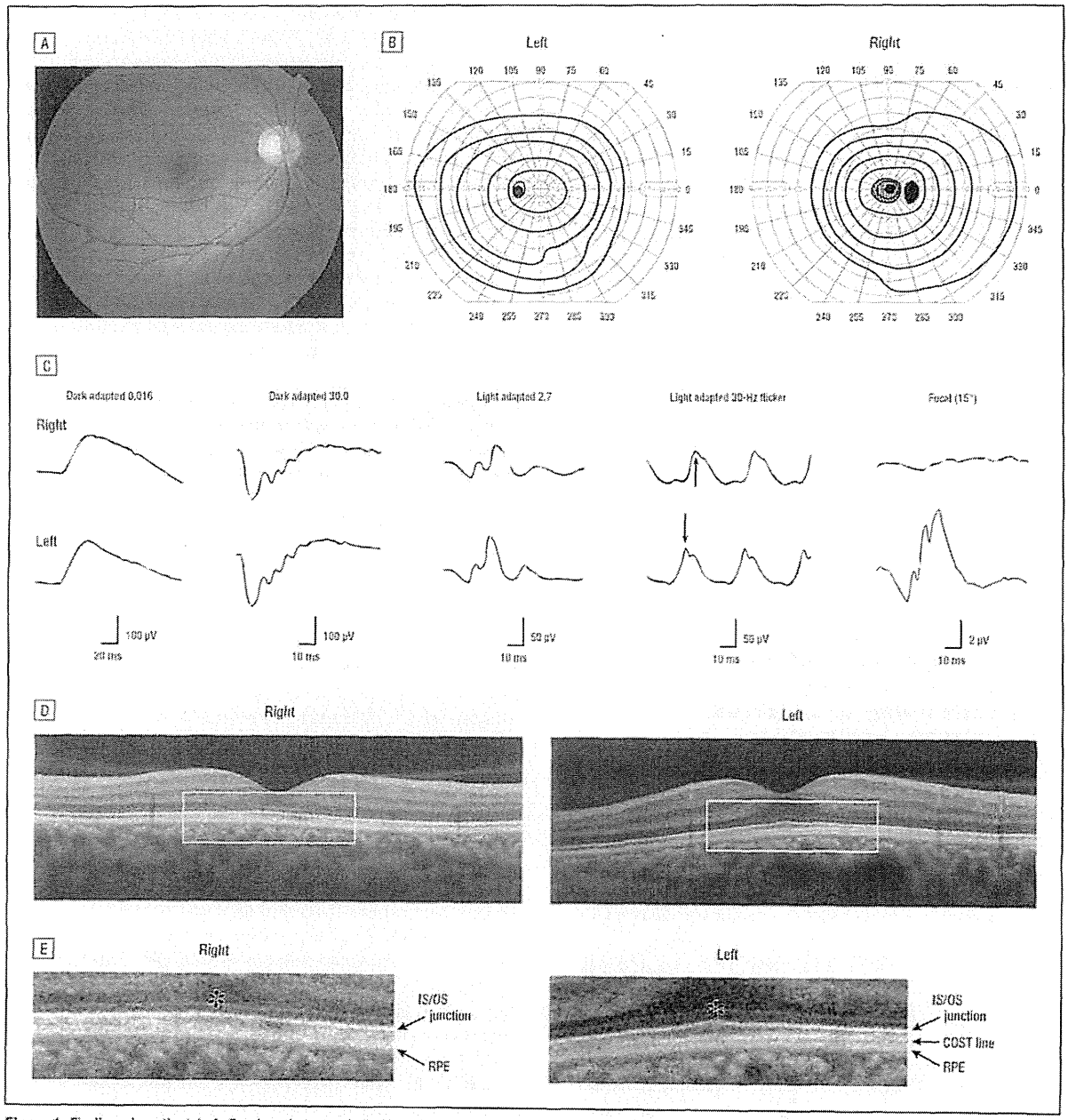


**Figure 1.** Findings in patient 1. A, Fundus photograph of the right eye showing a normal appearance. B, Goldmann kinetic perimetry showing a blind spot enlargement and central scotoma in the right eye. C, Full-field and focal macular electroretinograms. The latencies of the photopic 30-Hz flicker responses are delayed in the right eye. Arrows indicate the phase difference in light-adapted 30-Hz flicker responses. The focal macular electroretinogram is almost flat in the central 15° of the right eye. Optical coherence tomographic images vertically profiled along the foveola (D) and magnified optical coherence tomographic images in the region of visual field abnormality (E). In the left eye, the inner segment–outer segment (IS/OS) junction, foveal bulge, and cone OS tip (COST) line are clearly observed. In the right eye, the IS/OS junction is clearly observed but the COST line is absent in the macula. The foveal bulge (asterisk) cannot be observed in the right eye. RPE indicates retinal pigment epithelium.

Our findings suggest that the dysfunction of the cone photoreceptor OS could be initially reflected by an absence or indistinctness of the COST line and the absence of the foveal bulge.[3] These changes may be followed by the development of abnormalities in the IS/OS junction in the more advanced stages. However, in our cases, the IS/OS junction remained the same during the entire follow-up period. This may suggest another possibility that our 2 cases constitute a subtype of AZOOR. However, in another case of AZOOR with a blind spot enlargement and relative central scotoma (a 21-year-old woman, data not shown), both the IS/OS and COST lines disappeared in the peripapillary region where visual field disturbance was severe, whereas only the COST line disappeared and the IS/OS line remained normal in the foveal region where the visual field disturbance was milder. These findings support the idea that the visibility of the COST line is more easily affected than that of

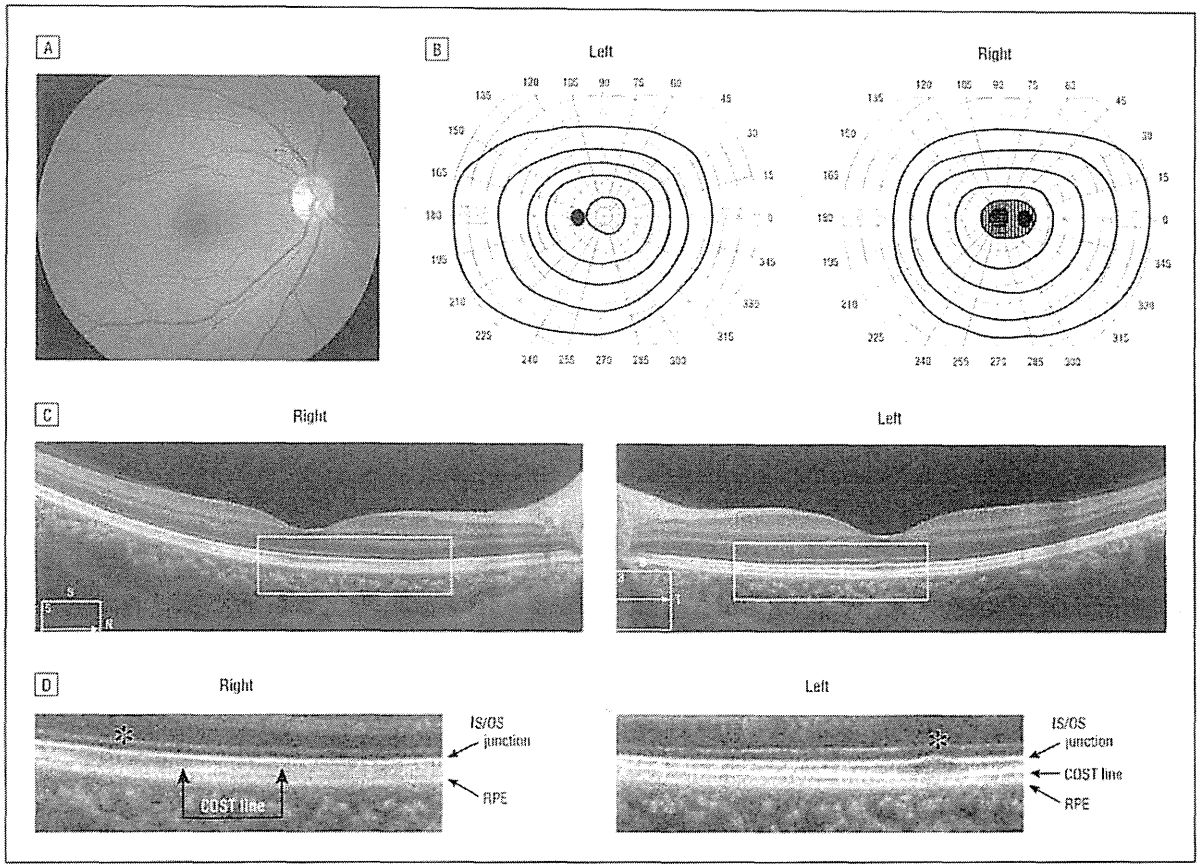


**Figure 2.** Findings in patient 2. A, Fundus photograph of the right eye showing a normal appearance. B, Goldmann kinetic perimetry showing a blind spot enlargement and central scotoma in the right eye. Optical coherence tomographic images horizontally profiled along the foveola (C), and magnified optical coherence tomographic images in the region of the visual field abnormality (D). In both eyes, the inner segment–outer segment (IS/OS) junction is clearly observed. In the right eye, the cone OS tip (COST) line is partially observed but appeared more indistinct than in the left eye. The foveal bulge (asterisk) cannot be seen in the right eye.

the IS/OS line at an earlier stage by the pathological changes in a typical case of AZOOR. We should note that care should be taken in evaluation of the COST line because its visibility is dependent on the intensity and direction of the laser light that reaches the photoreceptor layer.[6] However, in patients with AZOOR, the COST line and the foveal bulge observed by OCT could help as indicators of early cone photoreceptor dysfunction in cases with minimal ophthalmoscopic and angiographic abnormalities.

*Kazushige Tsunoda, MD*
*Kaoru Fujinami, MD*
*Yozo Miyake, MD*

**Author Affiliations:** National Institute of Sensory Organs, Tokyo (Drs Tsunoda and Fujinami), and Aichi Medical University, Aichi (Dr Miyake), Japan.
**Correspondence:** Dr Tsunoda, Laboratory of Visual Physiology, National Institute of Sensory Organs, 2-5-1 Higashigaoka, Meguroku, Tokyo 1528902, Japan (tsunodakazushige@kankakuki.go.jp).
**Financial Disclosure:** None reported.
**Funding/Support:** This work was supported by research grants from the Ministry of Health, Labor, and Welfare, Japan, and by SENTAN, Japan Science and Technology Agency, Japan.

1. Gass JD, Agarwal A, Scott IU. Acute zonal occult outer retinopathy: a long-term follow-up study. *Am J Ophthalmol*. 2002;134(3):329-339.
2. Li D, Kishi S. Loss of photoreceptor outer segment in acute zonal occult outer retinopathy. *Arch Ophthalmol*. 2007;125(9):1194-1200.
3. Zibrandtsen N, Munch IC, Klemp K, Jørgensen TM, Sander B, Larsen M. Photoreceptor atrophy in acute zonal occult outer retinopathy. *Acta Ophthalmol*. 2008;86(8):913-916.
4. Spaide RF, Koizumi H, Freund KB. Photoreceptor outer segment abnormalities as a cause of blind spot enlargement in acute zonal occult outer retinopathy-complex diseases. *Am J Ophthalmol*. 2008;146(1):111-120.
5. Takai Y, Ishiko S, Kagekawa H, Fukui K, Takahashi A, Yoshida A. Morphological study of acute zonal occult outer retinopathy (AZOOR) by multiplanar optical coherence tomography. *Acta Ophthalmol*. 2009;87(4):408-418.
6. Srinivasan VJ, Monson BK, Wojtkowski M, et al. Characterization of outer retinal morphology with high-speed, ultrahigh-resolution optical coherence tomography. *Invest Ophthalmol Vis Sci*. 2008;49(4):1571-1579.
7. Curcio CA, Sloan KR, Kalina RE, Hendrickson AE. Human photoreceptor topography. *J Comp Neurol*. 1990;292(4):497-523.

## Adult Ovarian Retinoblastoma Genomic Profile Distinct From Prior Childhood Eye Tumor

We report the first case of a woman, previously cured of childhood intraocular retinoblastoma, who developed tumor in the ovary with histological and genomic characteristics suggesting an independent retinoblastoma, not a metastasis.

addition, the duration of treatment to induce retinal reattachment is currently unknown. However, patients with IH have been treated for several months.

Hemangiomas consist histologically of cavernous and capillary vascular networks. The mechanism by which oral propranolol aids in the resolution of exudative retinal detachment in DCH associated with Sturge-Weber syndrome is unknown. It is possible that, similar to IH, there is vasoconstriction of the DCH due to decreased release of nitric oxide, blocking of proangiogenic signals including vascular endothelial growth factor and basic fibroblast growth factor, and apoptosis in proliferating endothelial cells with vascular tumor regression.[3]

To our knowledge, the benefits of propranolol therapy have not been reported in adult hemangioma or for DCH. This is the first reported case of propranolol treatment in an adult with exudative retinal detachment in DCH associated with Sturge-Weber syndrome.

*J. Fernando Arevalo, MD*
*Juan D. Arias, MD*
*Martin A. Serrano, MD*

Author Affiliations: Retina and Vitreous Service, Clínica Oftalmológica Centro Caracas, Caracas, Venezuela. Dr Arevalo is now with the Retina Division, Wilmer Eye Institute, Johns Hopkins University School of Medicine, Baltimore, Maryland, and the Vitreoretinal Division, King Khaled Eye Specialist Hospital, Riyadh, Saudi Arabia.
Correspondence: Dr Arevalo, Vitreoretinal Division, King Khaled Eye Specialist Hospital, Al-Oruba Street, PO Box 7191, Riyadh 11462, Saudi Arabia (arevalojf@jhmi.edu).
Financial Disclosure: None reported.
Funding/Support: This work was supported in part by the Arevalo-Coutinho Foundation for Research in Ophthalmology, Caracas, Venezuela.
Previous Presentation: This paper was presented at the 34th Annual Meeting of the Macula Society; March 9, 2011; Boca Raton, Florida.

1. Schilling H, Sauerwein W, Lommatzsch A, et al. Long-term results after low dose ocular irradiation for choroidal haemangiomas. *Br J Ophthalmol*. 1997; 81(4):267-273.
2. Anand R. Photodynamic therapy for diffuse choroidal hemangioma associated with Sturge Weber syndrome. *Am J Ophthalmol*. 2003;136(4):758-760.
3. Léauté-Labrèze C, Dumas de la Roque E, Hubiche T, Boralevi F, Thambo JB, Taïeb A. Propranolol for severe hemangiomas of infancy. *N Engl J Med*. 2008; 358(24):2649-2651.
4. Siegfried EC, Keenan WJ, Al-Jureidini S. More on propranolol for hemangiomas of infancy. *N Engl J Med*. 2008;359(26):2846.
5. Storch CH, Hoeger PH. Propranolol for infantile haemangiomas: insights into the molecular mechanisms of action. *Br J Dermatol*. 2010;163(2):269-274.
6. Sans V, de la Roque ED, Berge J, et al. Propranolol for severe infantile hemangiomas: follow-up report. *Pediatrics*. 2009;124(3):e423-e431.

## Oguchi Disease With Unusual Findings Associated With a Heterozygous Mutation in the *SAG* Gene

Oguchi disease is a type of congenital stationary night blindness with an autosomal recessive inheritance pattern. Two causative genes have been reported for Oguchi disease: the *SAG* and *GRK1* genes. Homozygous Oguchi disease is characterized by a golden-yellow discoloration of the fundus that disappears after prolonged dark adaptation, called the Mizuo-Nakamura phenomenon. The International Society for Clinical Electrophysiology of Vision–protocol bright-flash electroretinograms (ERGs), performed after 30 minutes of dark adaptation, are typically electronegative with a severely reduced b-wave and milder reduction of the a-wave.[1,2] After 3 to 4 hours of dark adaptation, both amplitudes recover to nearly normal, especially the a-wave.[2] However, the recovered rod function is rapidly lost after a short light exposure or a single bright white flash.[2,3]

We describe a case of Oguchi disease with unusual findings caused by a putative heterozygous mutation in the *SAG* gene.

Report of a Case. A 40-year-old woman with visual acuity of 20/20 OU had fundus abnormalities and was referred to our institute. She had photophobia but did not report night blindness. There was no autosomal dominant family history. The retina had a golden-yellow appearance (**Figure**, A). The Mizuo-Nakamura phenomenon was observed after 30 minutes of dark adaptation (Figure, B). Sequencing of the *SAG* gene identified a heterozygous mutation of 1147del A at codon 309. No mutation was found in *GRK1*.

The International Society for Clinical Electrophysiology of Vision protocol was used to record the ERGs. The scotopic ERGs after 30 minutes of dark adaptation showed slightly reduced amplitude and delayed implicit time in b-wave (Figure, C). The bright-flash ERG (30 candelas·seconds/m$^2$) had a positive configuration, although the b:a ratio was lower than normal (Figure, C). The photopic and flicker ERGs performed after 10 minutes of light adaptation were normal (Figure, C). To determine the extent of the rod function recovery, bright-flash ERGs were recorded 4 times at 30-second intervals after 30 minutes of dark adaptation. During the 4 stimuli, the waveform changed from the positive pattern to a negative configuration with a severely reduced b-wave and additional milder reduction of the a-wave, which is characteristic of homozygous Oguchi disease (Figure, D). To our knowledge, this phenomenon has never been reported in normal eyes, in eyes with the typical type of Oguchi disease, or in other cases of Oguchi disease with the same heterozygous *SAG* mutation (Figure, D). The superimposed ERGs elicited by the 4 consecutive flashes show the variation of rod function recovery (Figure, E).

Comment. To our knowledge, this is the first case of Oguchi disease with a distinct fundus appearance and mild electrophysiological abnormalities associated with a putative heterozygous *SAG* mutation. However, we cannot exclude the possibility that another mutation exists in the intron of another allele, which causes the mild phenotype in this patient.

The repetitive-flash ERG protocol was crucial for the diagnosis. It has been reported that double- or triple-flash stimulations after prolonged dark adaption induce ERG alterations in typical patients with Oguchi disease.[4] However, the use of a 30-second interval allowed us to follow the degree of rod function recovery.

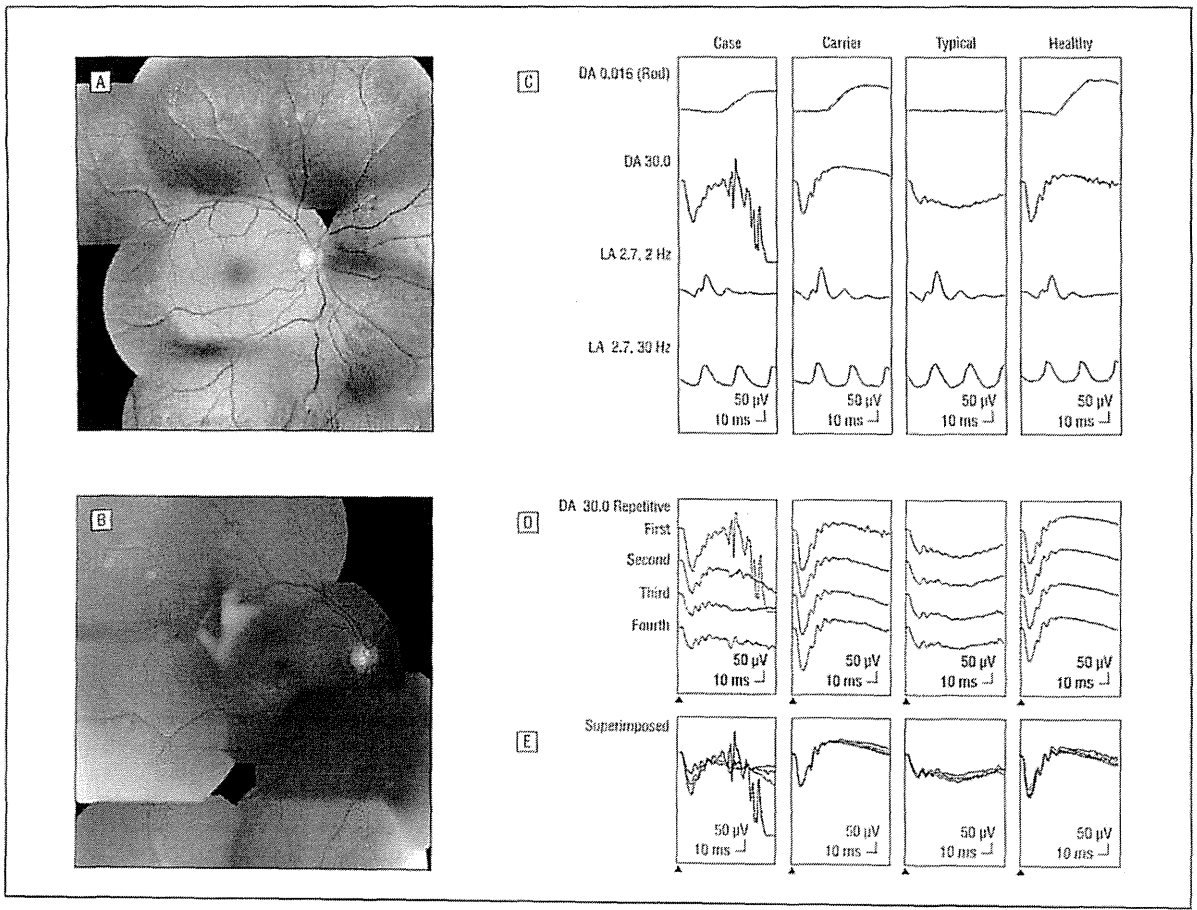


**Figure.** Fundus photographs showing the Mizuo-Nakamura phenomenon before (A) and after (B) 30 minutes of dark adaptation. C, The electroretinograms (ERGs) recorded according to the International Society for Clinical Electrophysiology of Vision protocol. D, The ERGs elicited by 4 repetitive flashes at interstimulus intervals of 30 seconds. E, Superimposed ERGs elicited by 4 flashes. The ERGs are from our patient with Oguchi disease (case), another patient with Oguchi disease with a heterozygous mutation (carrier), a typical patient with Oguchi disease, and a healthy subject. DA indicates dark adaptation; LA, light adaptation.

Arrestin and rhodopsin kinase act in sequence to deactivate rhodopsin to stop the phototransduction cascade.[4] Results of molecular biological studies have suggested that residual arrestin activity correlates with the severity of the clinical phenotype.[5] However, in our case it was more difficult to determine the relationship between the putative heterozygous mutation of the *SAG* gene and the mild electrophysiological abnormalities in the rod function recovery. A modifying effect of deactivating rhodopsin should be considered.

The time required for the reappearance of the rod function demonstrated in the electrophysiological study and the time required to demonstrate the Mizuo-Nakamura phenomenon were nearly identical. We suggest that the physiological basis for the Mizuo-Nakamura phenomenon may be closely related to the abnormal deactivation of rhodopsin.

*Kaoru Fujinami, MD*
*Kazushige Tsunoda, MD, PhD*
*Makoto Nakamura, MD, PhD*
*Yoshihisa Oguchi, MD, PhD*
*Yozo Miyake, MD, PhD*

**Author Affiliations:** Laboratory of Visual Physiology, National Institute of Sensory Organs, National Tokyo Medical Center (Drs Fujinami, Tsunoda, and Miyake) and Department of Ophthalmology, Keio University of Medicine (Dr Oguchi), Tokyo, and Department of Ophthalmology, Nagoya University Graduate School of Medicine, Aichi (Dr Nakamura), Japan.

**Correspondence:** Dr Tsunoda, Laboratory of Visual Physiology, National Institute of Sensory Organs, National Tokyo Medical Center, 2-5-1, Higashigaoka, Meguro-ku, Tokyo 152-8902, Japan (tsunodakazushige@kankakuki.go.jp).

**Financial Disclosure:** None reported.

1. Carr RE, Gouras P. Oguchi's disease. *Arch Ophthalmol*. 1965;73:646-656.
2. Miyake Y, Horiguchi M, Suzuki S, Kondo M, Tanikawa A. Electrophysiological findings in patients with Oguchi's disease. *Jpn J Ophthalmol*. 1996;40(4):511-519.
3. Gouras P. Electroretinography: some basic principles. *Invest Ophthalmol*. 1970;9(8):557-569.
4. Ohguro H, Van Hooser JP, Milam AH, Palczewski K. Rhodopsin phosphorylation and dephosphorylation in vivo. *J Biol Chem*. 1995;270(24):14259-14262.
5. Dryja TP. Molecular genetics of Oguchi disease, fundus albipunctatus, and other forms of stationary night blindness: LVII Edward Jackson Memorial Lecture. *Am J Ophthalmol*. 2000;130(5):547-563.

Retina

# Photoreceptor and Post-Photoreceptoral Contributions to Photopic ERG a-Wave in Rhodopsin P347L Transgenic Rabbits

*Rika Hirota,*[1,2] *Mineo Kondo,*[3] *Shinji Ueno,*[1] *Takao Sakai,*[1] *Toshiyuki Koyasu,*[1] *and Hiroko Terasaki*[1]

**Purpose.** The a-wave of the photopic electroretinogram (ERG) of macaque monkeys is made up of the electrical activities of cone photoreceptors and post-photoreceptoral neurons. However, it is not known whether the contributions of these two components change in retinas with inherited photoreceptor degeneration. The purpose of this study was to determine the contributions of cones and post-photoreceptoral neurons to the a-wave of the photopic ERGs in rhodopsin Pro347Leu transgenic (Tg) rabbits.

**Methods.** Ten Tg and 10 wild-type (WT) New Zealand White rabbits were studied at 4 and 12 months of age. The a-waves of the photopic ERGs were elicited by xenon flashes of different stimulus strengths before and after the activities of post-photoreceptoral neurons were blocked by intravitreal injections of a combination of 0.2 to 0.4 mM of 6-cyano-7-nitrouinoxaline-2,3(1H,4H)-dione, disodium (CNQX) and 2 to 4 mM of (±)-2-amino-4-phosphonobutyric acid.

**Results.** The percentage contribution of the cone photoreceptors to the photopic ERG a-waves increased with increasing stimulus strength, and the percentage ranged from 54% to 75% in 4-month-old WT rabbits. In contrast, the percentage contribution of the cone photoreceptors in 4-month-old Tg rabbits ranged from 32% to 51% ($P < 0.05$). The mean percentage contribution of cone photoreceptors became still smaller at 11% to 48% in 12-month-old Tg rabbits.

**Conclusions.** These results suggest that the relative contribution of cone photoreceptors to the photopic ERG a-wave is smaller in retinas with inherited photoreceptor degeneration. This indicates that the a-waves of the photopic ERGs in patients with retinitis pigmentosa must consider this lower contribution from the cone photoreceptors. (*Invest Ophthalmol Vis Sci.* 2012;53:1467–1472) DOI:10.1167/iovs.11-9006

The electroretinogram (ERG) is a mass electrical potential change of the retina that is elicited by light stimulation and is easily recorded noninvasively with a corneal electrode.[1] The ERG arises from the neural activity of the different types of retinal cells, and it can be used to perform a layer-by-layer study of retinal function in patients and animals.[2]

The origins of the photopic or light-adapted a-wave of the ERG in macaque monkeys was studied by Sieving et al.[3–5] They injected glutamate agonists and antagonists intravitreally to dissect the retinal circuits. They found that the a-wave of the photopic ERG received contributions not only from the cone photoreceptors but also from post-photoreceptoral neurons (e.g., OFF-bipolar cells and horizontal cells)[3,4] because *cis*-2,3-piperidine dicarboxylic acid (PDA) or kynurenic acid reduced the a-wave amplitude. A later study by Robson et al.[6] showed that the PDA-sensitive post-photoreceptoral a-wave component started at much earlier times of approximately 5 ms in macaques. Frieberg et al.[7] also estimated the time course of the cone photoreceptor response in normal human ERGs using the paired-flash technique, in which an intense "probe" flash was delivered at different times after a "test" flash. Their results showed that the photopic ERG a-wave of the human ERG contains an appreciable postphotoreceptoral component, similar to that reported in monkeys.[3–6]

These studies, which were designed to determine the origins of the photopic ERG a-wave, have been performed primarily on normal macaque monkeys and human eyes.[3–7] It is not known whether the contributions of photoreceptors and post-photoreceptoral neurons are altered in retinas with inherited photoreceptor degeneration (e.g., retinitis pigmentosa [RP]) because the most commonly used RP animals are mice and rats, whose amplitude of photopic ERG a-wave is very small. This makes it difficult to quantify the changes in the a-wave amplitude before and after intravitreal injection of pharmacologic agents.[8–12]

We have recently succeeded in generating a rabbit model of retinal degeneration.[13] This animal has the rhodopsin Pro347Leu mutation, which is one of the major mutations in autosomal dominant retinitis pigmentosa in humans.[14] These animals have a slowly progressive photoreceptor degeneration, as do human RP patients with this mutation,[13,15–18] though it is still unclear whether the retinal degeneration is due to a point mutation of the rhodopsin gene or to an overexpression of rhodopsin in these animals. We believed that this rhodopsin transgenic (Tg) rabbit can be an excellent animal model in which to study the retinal origins of the photopic ERG a-wave in RP because rabbits have a large photopic a-wave. In addition, the large size of the rabbit's eye enabled us to perform reliable intravitreal injections of pharmacologic agents.[15,16,18]

Thus, the purpose of this study was to compare the contributions of cone photoreceptors and post-photoreceptoral neurons with the a-wave of the photopic ERGs between wild-type (WT) and Tg rabbits. To accomplish this we examined the postphotoreceptoral neural activity before and after they were blocked by pharmacologic agents.

From the [1]Department of Ophthalmology, Nagoya University Graduate School of Medicine, Nagoya, Japan; the [2]Drug Safety Research Laboratories, Astellas Pharma Inc., Osaka, Japan; and the [3]Department of Ophthalmology, Mie University Graduate School of Medicine, Tsu, Japan.

Supported by Grant-in-Aid for Scientific Research B (203904480) and Grant-in-Aid for Scientific Research C (20592075) from the Ministry of Education, Culture, Sports, Science and Technology, Japan.

Submitted for publication November 3, 2011; revised January 13, 2012; accepted January 14, 2012.

Disclosure: **R. Hirota**, Astellas Pharma Inc. (E); **M. Kondo**, None; **S. Ueno**, None; **T. Sakai**, None; **T. Koyasu**, None; **H. Terasaki**, None

Corresponding author: Mineo Kondo, Department of Ophthalmology, Mie University Graduate School of Medicine, 2-174 Edobashi, Tsu 514-8507, Japan; mineo@clin.medic.mie-u.ac.jp.

## Materials and Methods

### Animals

The experiments were performed on 10 Tg and 10 littermate WT New Zealand White rabbits. Our techniques for generating Tg rabbits have been described in detail.[15] This study was conducted in accordance with the ARVO Statement for the Use of Animals in Ophthalmic and Vision Research. All protocols were approved by the Animal Research Review Board of Nagoya University Graduate School of Medicine (no. 23005).

### ERG Recordings

Each animal was anesthetized with an intramuscular injection of 25 mg/kg ketamine and 2 mg/kg xylazine. ERGs were recorded with a bipolar contact lens electrode (GoldLens; Doran Instruments, Littleton, MA). Animals were placed in a Ganzfeld bowl and stimulated with stroboscopic stimuli (model SG-2002; LKC Technologies, Gaithersburg, MD). The full-strength stimulus was attenuated with neutral density filters in 0.5-log unit steps. Photopic ERGs were recorded after 10 minutes of light adaptation, and the stimulus strength ranged from 0.2 to 2.2 log cd-s/m$^2$ (photopic unit), and they were presented on a rod-suppressing white background of 3.3 log scot td. Signals were amplified, band pass-filtered between 0.3 to 1000 Hz, and averaged using a computer-assisted signal analysis system (MEB-9100; Neuropack, Nihon Kohden, Tokyo, Japan).

### Drug Injections

Drugs and techniques for the intravitreal injections have been described in detail.[15,16,18] The drugs were dissolved in sterile PBS, and the pH was titrated to 7.4 with hydrochloric acid or sodium hydrate. The drugs were injected into the vitreous with a 30-gauge needle inserted through the pars plana approximately 1 mm posterior to the limbus.

Two types of glutamate analogs—(±)-2 amino-4-phosphonobutyric acid (APB; Sigma-Aldrich Japan, Tokyo, Japan) and 6-cyano-7-nitroquinoxaline-2,3(1H,4H)-dione (CNQX, Sigma-Aldrich Japan)—were used. APB is an agonist of the type 6 metabotropic glutamate receptor, and it blocks signal transmission between the photoreceptors and depolarizing or ON-bipolar cells.[19] CNQX is an antagonist of the α-amino-3-hydroxy-5-methyl-4-isoxazolepropionic acid/kainic acid (AMPA/KA) class of ionotropic glutamate receptors and is known to block the light responses of the hyperpolarizing or OFF-bipolar cells, horizontal cells, and all third-order retinal neurons.[20] Thus, the combination of APB and CNQX is expected to isolate the photoreceptor responses. We could not use PDA,[21] another type of antagonist of the AMPA/KA class of ionotropic glutamate receptors, because PDA was not commercially available. Intravitreal concentrations were 2 to 4 mM for APB and 0.2 to 0.4 mM for CNQX, assuming that the vitreous volume of the NZW rabbit is 1.5 mL.[22] The drugs were dissolved in 0.05 mL saline.

Recordings were begun approximately 60 to 90 minutes after the drug injections, and studies were completed within 3 hours. Although the drug effects were reversible, we only used the rabbits that had not been used for any previous experiments.

### Measurement of a-Waves

To determine the photoreceptor and post-photoreceptoral contributions to the a-wave of the photopic ERGs quantitatively, we measured the amplitude of the a-wave before and after drug administration. Before drug administration, the a-wave amplitude was measured from the baseline to the first negative trough; after it, the a-wave amplitude was measured from the baseline to the potential at the time of the a-wave peak before the drugs (Fig. 1A). Then the percentage cone photoreceptor contribution was calculated by the expression (a-wave amplitude after APB and CNQX)/(a-wave amplitude before drugs) × 100. This method has been used to determine the degree of cone photoreceptor contribution to the a-wave.[3]

### Statistical Analysis

Because the data were normally distributed, unpaired Student's *t*-tests were used to determine whether the amplitude of the a-wave of WT rabbits was significantly different from that of Tg rabbits. Differences were considered to be significant when $P < 0.05$.

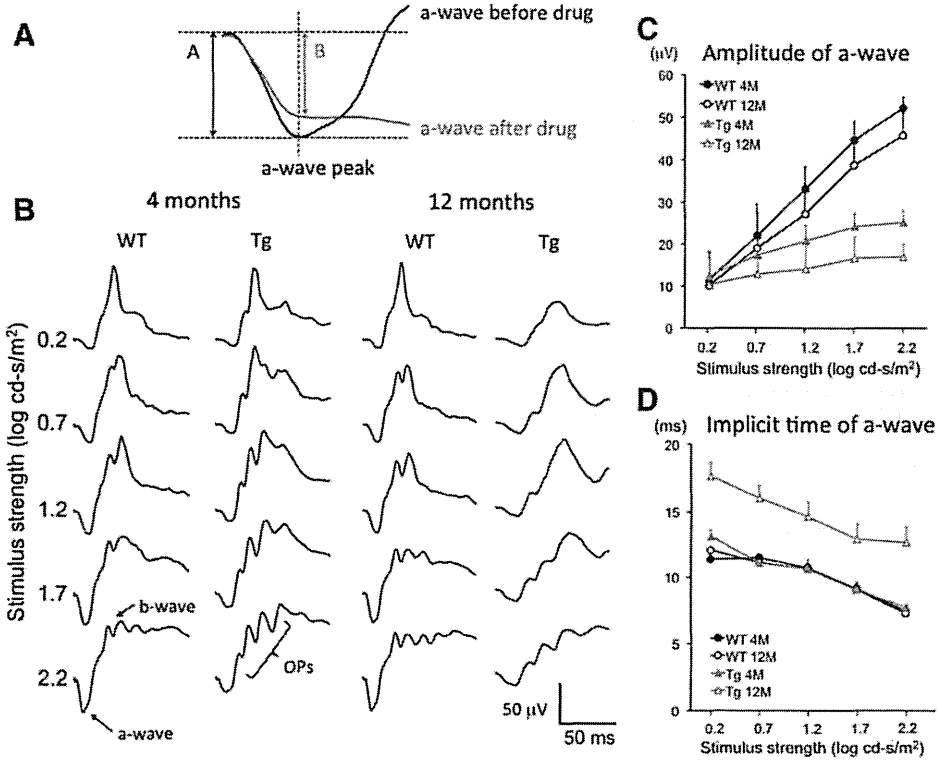


FIGURE 1. Photopic ERGs of WT and rhodopsin P347L Tg rabbits. (A) Method of measuring a-wave amplitude. The a-wave amplitude before drug administration was measured from the baseline to the first negative trough. (B) The a-wave amplitude after drug administration was measured from the baseline to the negative value at the time of the a-wave peak before drug administration. Representative photopic ERGs recorded from WT and Tg rabbits at 4 and 12 months of age. ERG waveforms to five different stimulus strengths of 0.2 to 2.2 log cd-s/m$^2$ are shown. (C) Plots of the a-wave amplitude to five different stimulus strengths. Results of WT and Tg rabbits at 4 and 12 months of age are shown. Bars indicate the SE of the means of five animals. (D) Plots of the a-wave implicit times to five different stimulus strengths. Results of WT and Tg rabbits at 4 and 12 months of age are shown. Bars indicate the SE of the means of five animals.

## Results

### Photopic ERGs of WT and Tg Rabbits

Representative photopic ERGs recorded from WT and Tg rabbits at 4 and 12 months of age are shown in Figure 1B. The ERG waveforms elicited by five different stimulus strengths from 0.2 to 2.2 log cd-s/m$^2$ are shown. We found that all the ERG components of Tg rabbits decreased progressively with increasing age; the a-wave was more affected than the b-wave. These general ERG findings agree with the results reported in our earlier publications.[13,15]

The amplitudes of the a-waves of the photopic ERGs of Tg rabbits were significantly smaller than those of WT rabbits at 4 months of age and even smaller at 12 months of age (Figs. 1B, 1C). The implicit times of the photopic ERG a-wave were not significantly different between the Tg and WT rabbits when they were 4 months of age, but the Tg rabbits had severely delayed implicit times when they were 12 months of age (Fig. 1D).

### Effect of APB or CNQX Alone on Photopic ERG a-Wave

To confirm that the a-waves of the photopic ERG in rabbits originated from the same neurons as macaque monkeys, we examined the effect of APB or CNQX alone on the a-wave of the photopic ERGs in WT and Tg rabbits when they were 4 months of age (Fig. 2). We found that intravitreal injection of APB did not alter the leading edge of the photopic a-wave, and the maximal a-wave amplitudes were nearly the same before and after the APB injection for both WT and Tg rabbits (Fig. 2, upper trace). In contrast, an intravitreal injection of CNQX significantly changed the leading edge of the a-wave, and the maximal a-wave amplitude was significantly reduced in both types of rabbits (Fig. 2, lower trace). These results were comparable to the results in primates[3–6] and support the belief that the photopic ERG a-wave receives significant contributions from post-photoreceptoral neurons, including OFF-bipolar cells and horizontal cells in both WT and Tg rabbits.

### Amplitude Changes of Photopic ERG a-Wave after Pharmacologic Drug Administration

We next examined the contribution of the cone photoreceptors to the photopic ERG a-wave at the time of the a-wave peak. The black lines in Figure 3 show the photopic ERG a-waves before drugs, and the color lines (blue, WT; red, Tg) show the ERG waveforms after intravitreal injection of a solution of combined APB and CNQX (i.e., the cone photoreceptor response). The vertical dotted lines show the timing of the a-wave peaks before drug administration. As reported in primates,[3–6] the a-wave amplitude is greatly reduced after blocking all post-photoreceptoral neurons by glutamate analogs.

Mean amplitudes of the a-wave before and after drug administration at the time of the a-wave peak (Fig. 1A), are plotted in Figure 4. The a-wave amplitude decreased after injection of both APB and CNQX for all stimulus strengths in both WT and Tg rabbits.

### Relative Contributions of Cone Photoreceptors to Photopic a-Wave

We next compared the relative contributions of the cone photoreceptors with the photopic ERG a-wave for the two types of rabbits. For this, we calculated the percentage contribution of the cone photoreceptors; that is, we divided the a-wave amplitude after APB+CNQX by the a-wave amplitude before drug administration (Fig. 5). We found that the percentage contribution of the cone photoreceptors became greater with increasing stimulus strengths in both WT and Tg rabbits, which is consistent with the findings in normal macaque monkeys.[3] The percentage contribution of the cone photoreceptors ranged from 32% to 51% in Tg rabbits, which was significantly smaller than that in WT rabbits at 54% to 75%, at 4 months of age ($P < 0.01$; Fig. 5, left).

We also calculated these values when the animals were 12 months of age. The percentage contribution of the cone photoreceptors ranged from 11% to 48% in Tg rabbits, which was also significantly smaller than that in WT rabbits at 41% to 70% ($P < 0.05$; Fig. 5, right). The percentage contribution of cone

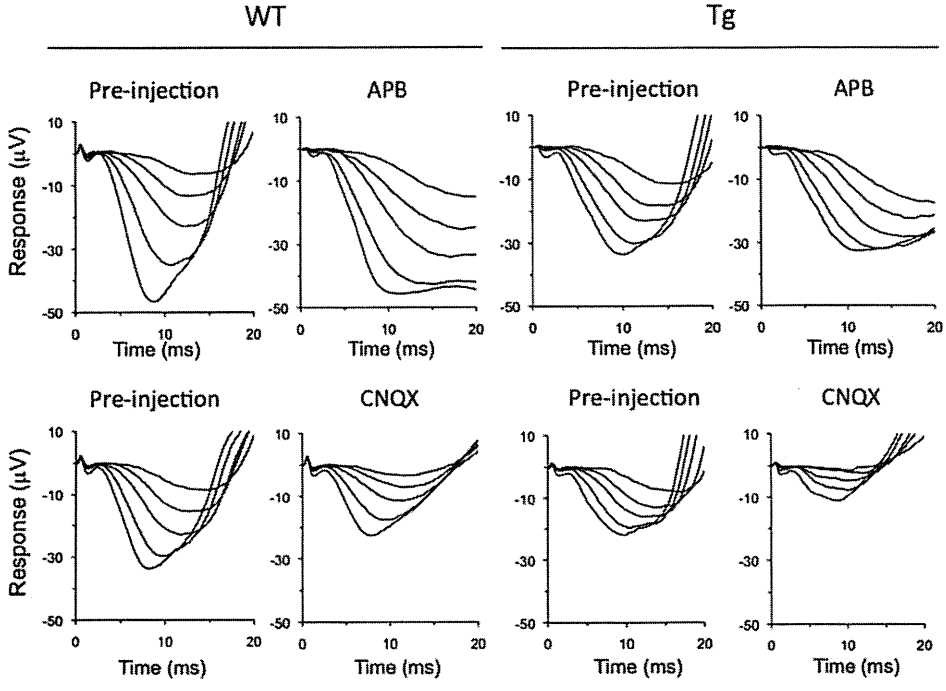


FIGURE 2. Representative waveforms of photopic ERG a-wave before and after APB or CNQX alone in WT and Tg rabbits of 4 months of age. ERG waveforms to five different stimulus strengths of 0.2 to 2.2 log cd-s/m$^2$ are superimposed.

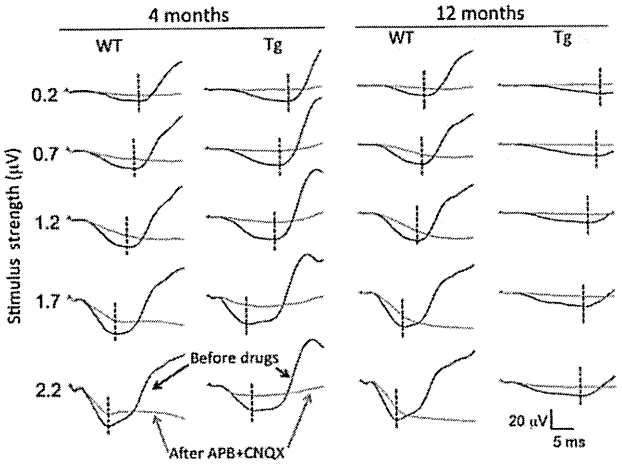


FIGURE 3. Representative waveforms of photopic ERG a-wave before (*black*) and after (*blue* and *red*) intravitreal injection of combination of APB and CNQX in WT and Tg rabbits at 4 and 12 months of age. *Vertical dotted lines*: timing of the a-wave peaks before drug administration.

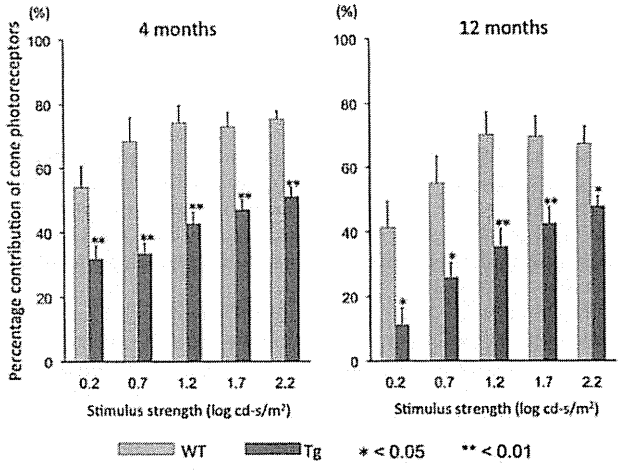


FIGURE 5. Plots of the percentage contribution of cone photoreceptors to the photopic ERG a-wave in WT (*blue*) and Tg (*red*) rabbits at 4 and 12 months of age. Bars indicate the SE of the means of five animals. $^*P < 0.05$; $^{**}P < 0.01$.

photoreceptors to the photopic a-wave in 12-month-old Tg rabbits was <50% for all stimulus strengths.

## Comparison of Postreceptoral Components

The smaller contributions of cone photoreceptors to the photopic a-waves in Tg rabbits can be explained simply by a decrease in cone photoreceptor responses caused by the photoreceptor degenerations, which can be clearly seen in Figure 4. However, it can also be caused by an increase in neural activities of the post-photoreceptoral neurons. To investigate whether the latter explanation was the cause, we calculated the amplitudes of post-photoreceptoral components at the time of the a-wave peak by subtracting the post-APB+CNQX waveform from the predrug waveform. Results are plotted in Figure 6.

Although the maximal amplitudes of the post-photoreceptoral components were not significantly different in WT and Tg rabbits, the intensity amplitude function for the two types of rabbits were different when they were 4 months of age (Fig. 6, left). The amplitude of the post-photoreceptoral component was nearly saturated at lower stimulus strengths of 0.7 to 1.2 log cd-s/m$^2$ in Tg rabbits. In contrast, this value increased gradually and reached maximum amplitude at the highest stimulus strength of 2.2 log cd-s/m$^2$ in WT rabbits. The amplitudes of the post-photoreceptoral components in Tg rabbits were significantly larger than those in WT rabbits at lower stimulus strengths of 0.2 and 0.7 log cd-s/m$^2$ ($P < 0.05$).

A similar tendency of the stimulus strength-amplitude functions of WT and Tg rabbits was also seen when they were 12 months of age, but the overall amplitudes of post-photoreceptoral components of Tg rabbits were greatly reduced, probably because of advanced retinal degeneration. These results indicated that the smaller contribution of cone photoreceptors to the photopic a-wave in young Tg rabbits occurred partially because of the enhanced post-photoreceptoral responses at lower stimulus strengths.

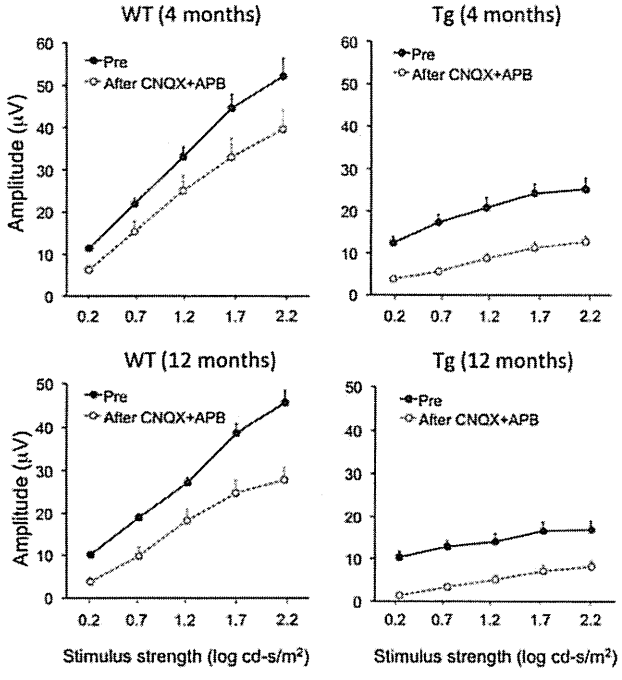


FIGURE 4. Plots of the a-wave amplitude before (*black*) and after (*blue* and *red*) intravitreal injection of combination of APB and CNQX in WT (*left*) and Tg (*right*) rabbits at 4 and 12 months of age. Bars indicate the SE of the means of five animals.

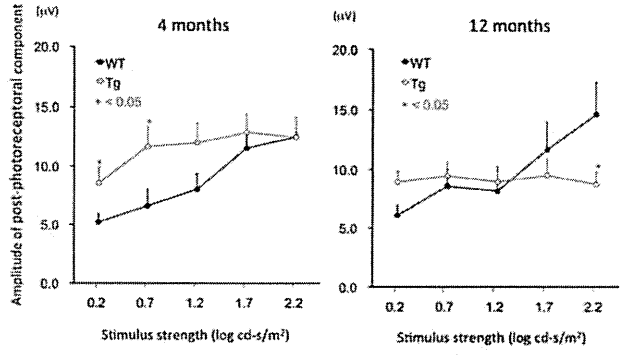


FIGURE 6. Plots of the amplitude of post-photoreceptoral component in the photopic ERG a-wave in WT (*black*) and Tg (*red*) rabbits at 4 and 12 months of age. Bars indicate the SE of the means of five animals. $^*P < 0.05$.

## Discussion

It is unknown whether the contributions of photoreceptors and post-photoreceptoral neurons are altered in retinas with progressive photoreceptor degeneration. Our present results clearly demonstrated that the percentage contribution of the cone photoreceptors to the photopic a-wave was significantly lower in rhodopsin P347L Tg rabbits than in WT rabbits over a 2 log unit range of stimulus strengths at both 4 and 12 months of age. We found that especially in the retina of 12-month-old Tg rabbits, the percentage contribution of cone photoreceptor to the photopic ERG a-wave was less than half, irrespective of the stimulus strength (Fig. 5, right).

Our results showed that the effects of stimulus strength on the cone photoreceptors and post-photoreceptoral contributions to the photopic a-wave of normal retinas were similar to those in primates reported by Bush and Sieving.[3] They measured the degree of cone photoreceptor and post-photoreceptoral contribution to the photopic a-wave at the time of the a-wave peak in normal macaque monkeys before and after APB and PDA. They did not report the exact percentage values, but they showed[3] that it was relatively low at 55% at the lowest stimulus strengths and that it gradually increased to a maximum of 92% at the highest stimulus strength. They interpreted these findings that the post-photoreceptoral contribution to the photopic a-wave was primarily responsible for the initial 1 to 1.5 log units of strength, whereas cone photoreceptor contribution progressively dominated the photopic a-wave at higher stimulus strengths. We also observed a similar pattern in our WT rabbits (Fig. 5), but the percentage contribution of cone photoreceptor at the highest stimulus strength was higher in macaque (92%) than in our WT rabbits (75%). This difference might have been due to the difference in the type of stimulus (200-ms long-flash stimuli in their study vs. xenon brief-flash stimuli in our study) or difference in species.

We found that the percentage contribution of cone photoreceptors to the photopic a-wave in Tg rabbits was significantly lower than in WT rabbits (Fig. 5). These results are reasonable because the cone photoreceptor is gradually attenuated whereas the middle and inner retinas are still well preserved in Tg rabbits.[13,15] Additional analyses demonstrated that the smaller percentage contribution of cone photoreceptors in young Tg rabbits can be explained, in part, by the enhancement of the amplitudes of the post-photoreceptoral component, especially at lower stimulus strengths (Fig. 6, left). Such enhanced amplitudes of the post-photoreceptoral component in Tg rabbits were no longer present at 12 months in Tg rabbits, probably because of advanced retinal degeneration.

We do not know the exact mechanism for the enhanced amplitudes of the post-photoreceptoral components elicited by weaker stimulus intensities in young Tg rabbits. This enhanced post-photoreceptoral response may be due to secondary functional changes in the OFF-bipolar/horizontal cells or their synapses after progressive photoreceptor degenerations.

Using computational molecular phenotyping, we have recently shown that during the course of rod photoreceptor degeneration, rod ON-bipolar cells switch their phenotype by expressing ionotropic glutamate receptors (iGluRs).[17] We also found that the rod bipolar cells effectively lose rod contacts and make ectopic cone contacts and express iGluRs.[17] This secondary retinal remodeling may contribute to the enhanced post-photoreceptoral responses in our Tg rabbits. Similarly, detailed ERG studies in rhodopsin P347L Tg pigs and rabbits have demonstrated that the electrical activities of the cone ON-pathway were also enhanced at a relatively early stage of retinal degeneration.[18,23] In addition, an increase in the ERG responses from the inner retina (e.g., scotopic threshold response) was also reported in the retina of the aged Royal College of Surgeons rat, a rodent model of retinal degeneration.[24,25]

Taken together, inherited retinal diseases associated with progressive photoreceptor degeneration may lead to different types of functional changes in the post-photoreceptoral retinal circuits, including the ON- and OFF pathways, during a relatively early stage of retinal degeneration.

We believe our results have important clinical implications. The a-wave of the photopic ERG is believed to be shaped primarily by electrical activities of cone photoreceptors in patients. However, the results of this study suggest that the cone photoreceptor function may be overestimated when the amplitude of the cone ERG a-wave is used as an indicator of residual cone photoreceptor functions in patients with progressive photoreceptor degeneration such as RP. Thus, when the standard stimulus strength (3.0 cd-s/m$^2$ = 0.48 log cd-s/m$^2$) recommended by the International Society of Clinical Electrophysiology of Vision[1] was used, contributions of the cone photoreceptors to the photopic a-wave was only 34% at the time of the a-wave peak, and the other 66% originated from post-photoreceptoral neurons (Fig. 5, left). Our results suggest that the lower contribution of the cones to the a-waves of the photopic ERGs must be considered in patients with RP.

There are limitations to this study. One was that we assessed the contribution of photoreceptors and post-photoreceptoral components only at the time of the a-wave peak before the drugs. However, the peak time of the a-wave depends on not only the stimulus strength but also on the presence of retinal degeneration (Fig. 1D). In addition, the a-wave can be truncated by the b-wave. To overcome this, we measured the a-wave amplitude at specific times before the b-wave intrusion (10.5 ms for 0.2 log cd-s/m$^2$, 9.5 ms for 0.7 log cd-s/m$^2$, 8.5 ms for 1.2 log cd-s/m$^2$, 7.5 ms for 1.7 log cd-s/m$^2$, and 6.5 ms for 2.2 log cd-s/m$^2$), and calculated the percentage cone photoreceptor contribution when the animals were 4 months of age. We found that the cone photoreceptor contribution still tended to be smaller in Tg rabbits than in WT rabbits, and the differences were significant at the two lower stimulus strengths ($P < 0.01$, Supplementary Fig. S1A, http://www.iovs.org/lookup/suppl/doi:10.1167/iovs.11-9006/-/DCSupplemental). We also measured the a-wave amplitude at a single constant time of 7 ms and calculated the percentage cone photoreceptor contribution. Again, the cone photoreceptor contribution tended to be smaller in Tg rabbits than in WT rabbits, but the difference was significant only at the highest stimulus strength (Supplementary Fig. S1B, http://www.iovs.org/lookup/suppl/doi:10.1167/iovs.11-9006/-/DCSupplemental).

In summary, our results indicate that the relative contribution of cone photoreceptors to the photopic ERG a-wave is smaller in retinas with inherited photoreceptor degeneration. These results suggest that care must be taken in interpreting the a-wave amplitudes of photopic ERGs in patients with progressive photoreceptor degeneration.

### Acknowledgments

The authors thank Duco I. Hamasaki for editing the manuscript and Michael Bach for helpful discussions.

### References

1. Marmor MF, Fulton AB, Holder GE, et al. ISCEV Standard for full-field clinical electroretinography (2008 update). *Doc Ophthalmol.* 2009;118:69–77.
2. Frishman LJ. Origins of the electroretinogram. In: Heckenlively JR, Arden GB, eds. *Principles and Practice of Clinical Electrophysiology of Vision.* 2nd ed. London: MIT Press; 2006:139–183.
3. Bush RA, Sieving PA. A proximal retinal component in the primate photopic ERG a-wave. *Invest Ophthalmol Vis Sci.* 1994;35:635–645.

4. Sieving PA, Murayama K, Naarendorp F. Push-pull model of the primate photopic electroretinogram: a role for hyperpolarizing neurons in shaping the b-wave. *Vis Neurosci.* 1994;11:519–532.
5. Jamison JA, Bush RA, Lei B, Sieving PA. Characterization of the rod photoresponse isolated from the dark-adapted primate ERG. *Vis Neurosci.* 2001;18:445–455.
6. Robson JG, Saszik SM, Ahmed J, Frishman LJ. Rod and cone contributions to the a-wave of the electroretinogram of the macaque. *J Physiol.* 2003;547:509–530.
7. Friedburg C, Allen CP, Mason PJ, Lamb TD. Contribution of cone photoreceptors and post-receptoral mechanisms to the human photopic electroretinogram. *J Physiol.* 2004;556:819–834.
8. Sharma S, Ball SL, Peachey NS. Pharmacological studies of the mouse cone electroretinogram. *Vis Neurosci.* 2005;22:631–636.
9. Bui BV, Fortune B. Origin of electroretinogram amplitude growth during light adaptation in pigmented rats. *Vis Neurosci.* 2006;23:155–67.
10. Koyasu T, Kondo M, Miyata K, et al. Photopic electroretinograms of mGluR6-deficient mice. *Curr Eye Res.* 2008;33:91–99.
11. Miura G, Wang MH, Ivers KM, Frishman LJ. Retinal pathway origins of the pattern ERG of the mouse. *Exp Eye Res.* 2009;89:49–62.
12. Shirato S, Maeda H, Miura G, Frishman LJ. Postreceptoral contributions to the light-adapted ERG of mice lacking b-waves. *Exp Eye Res.* 2008;86:914–928.
13. Kondo M, Sakai T, Komeima K, et al. Generation of a transgenic rabbit model of retinal degeneration. *Invest Ophthalmol Vis Sci.* 2009;50:1371–1377.
14. Dryja TP, Hahn LB, Cowley GS, et al. Mutation spectrum of the rhodopsin gene among patients with autosomal dominant retinitis pigmentosa. *Proc Natl Acad Sci U S A.* 1991;88:9370–9374.
15. Sakai T, Kondo M, Ueno S, et al. Supernormal ERG oscillatory potentials in transgenic rabbit with rhodopsin P347L mutation and retinal degeneration. *Invest Ophthalmol Vis Sci.* 2009;50:4402–449.
16. Yokoyama D, Machida S, Kondo M, et al. Pharmacological dissection of multifocal electroretinograms of rabbits with Pro347Leu rhodopsin mutation. *Jpn J Ophthalmol.* 2010;54:458–466.
17. Jones BW, Kondo M, Terasaki H, et al. Retinal remodeling in the Tg P347L rabbit, a large-eye model of retinal degeneration. *J Comp Neurol.* 2011;519:2713–2733.
18. Nishimura T, Machida S, Kondo M, et al. Enhancement of ON-bipolar cell responses of cone electroretinograms in rabbits with Pro347Leu rhodopsin mutation. *Invest Ophthalmol Vis Sci.* 2011;52:7610–7617.
19. Slaughter MM, Miller RF. 2-Amino-4-phosphonobutyric acid: a new pharmacological tool for retina research. *Science.* 1981;211:182–185.
20. Honoré T, Davies SN, Drejer J, et al. Quinoxalinediones: potent competitive non-NMDA glutamate receptor antagonists. *Science.* 1988;241:701–703.
21. Slaughter MM, Miller RF. An excitatory amino acid antagonist blocks cone input to sign-conserving second-order retinal neurons. *Science.* 1983;219:1230–1232.
22. Leeds JM, Henry SP, Truong L, et al. Pharmacokinetics of a potential human cytomegalovirus therapeutic, a phosphorothioate oligonucleotide, after intravitreal injection in the rabbit. *Drug Metab Dispos.* 1997;25:921–926.
23. Banin E, Cideciyan AV, Alemán TS, et al. Retinal rod photoreceptor-specific gene mutation perturbs cone pathway development. *Neuron.* 1999;23:549–557.
24. Bush RA, Hawks KW, Sieving PA. Preservation of inner retinal responses in the aged Royal College of Surgeons rat: evidence against glutamate excitotoxicity in photoreceptor degeneration. *Invest Ophthalmol Vis Sci.* 1995;36:2054–2062.
25. Machida S, Raz-Prag D, Fariss RN, et al. Photopic ERG negative response from amacrine cell signaling in RCS rat retinal degeneration. *Invest Ophthalmol Vis Sci.* 2008;49:442–452.

OPEN ACCESS Freely available online

PLoS one

# Identification of Autoantibodies against TRPM1 in Patients with Paraneoplastic Retinopathy Associated with ON Bipolar Cell Dysfunction

**Mineo Kondo[1*9], Rikako Sanuki[2,3☯], Shinji Ueno[1], Yuji Nishizawa[4], Naozumi Hashimoto[5], Hiroshi Ohguro[6], Shuichi Yamamoto[7], Shigeki Machida[8], Hiroko Terasaki[1], Grazyna Adamus[9], Takahisa Furukawa[2,3*]**

1 Department of Ophthalmology, Nagoya University Graduate School of Medicine, Nagoya, Aichi, Japan, 2 Department of Developmental Biology, Osaka Bioscience Institute, Suita, Osaka, Japan, 3 JST, CREST, Suita, Osaka, Japan, 4 Department of Biomedical Sciences, Chubu University, Kasugai, Aichi, Japan, 5 Department of Respiratory Medicine, Nagoya University Graduate School of Medicine, Nagoya, Aichi, Japan, 6 Department of Ophthalmology, Sapporo Medical University School of Medicine, Sapporo, Hokkaido, Japan, 7 Department of Ophthalmology and Visual Science, Chiba University Graduate School of Medicine, Chiba, Chiba, Japan, 8 Department of Ophthalmology, Iwate Medical University School of Medicine, Morioka, Iwate, Japan, 9 Department of Ophthalmology, Oregon Health and Science University, Portland, Oregon, United States of America

## Abstract

*Background:* Paraneoplastic retinopathy (PR), including cancer-associated retinopathy (CAR) and melanoma-associated retinopathy (MAR), is a progressive retinal disease caused by antibodies generated against neoplasms not associated with the eye. While several autoantibodies against retinal antigens have been identified, there has been no known autoantibody reacting specifically against bipolar cell antigens in the sera of patients with PR. We previously reported that the transient receptor potential cation channel, subfamily M, member 1 (TRPM1) is specifically expressed in retinal ON bipolar cells and functions as a component of ON bipolar cell transduction channels. In addition, this and other groups have reported that human TRPM1 mutations are associated with the complete form of congenital stationary night blindness. The purpose of the current study is to investigate whether there are autoantibodies against TRPM1 in the sera of PR patients exhibiting ON bipolar cell dysfunction.

*Methodology/Principal Findings:* We performed Western blot analysis to identify an autoantibody against TRPM1 in the serum of a patient with lung CAR. The electroretinograms of this patient showed a severely reduced ON response with normal OFF response, indicating that the defect is in the signal transmission between photoreceptors and ON bipolar cells. We also investigated the sera of 26 patients with MAR for autoantibodies against TRPM1 because MAR patients are known to exhibit retinal ON bipolar cell dysfunction. Two of the patients were found to have autoantibodies against TRPM1 in their sera.

*Conclusion/Significance:* Our study reveals TRPM1 to be one of the autoantigens targeted by autoantibodies in at least some patients with CAR or MAR associated with retinal ON bipolar cell dysfunction.

**Citation:** Kondo M, Sanuki R, Ueno S, Nishizawa Y, Hashimoto N, et al. (2011) Identification of Autoantibodies against TRPM1 in Patients with Paraneoplastic Retinopathy Associated with ON Bipolar Cell Dysfunction. PLoS ONE 6(5): e19911. doi:10.1371/journal.pone.0019911

**Editor:** Steven Barnes, Dalhousie University, Canada

**Received** February 10, 2011; **Accepted** April 6, 2011; **Published** May 17, 2011



**Funding:** This work was supported by CREST from the Japan Science and Technology Agency (http://www.jst.go.jp/), and a Grant-in-Aid for Scientific Research (B)(C) (#20390448, #20390087, #20592075, #20791678) from the Ministry of Education, Culture, Sports, Science and Technology (http://www.jsps.go.jp/), the Takeda Science Foundation (http://www.takeda-sci.or.jp/), The Uehara Memorial Foundation (http://www.ueharazaidan.com/), the Naito Foundation (http://www.naito-f.or.jp/), the Novartis Foundation (#20-10, http://novartisfound.or.jp/), Mochida Memorial Foundation for Medical and Pharmaceutical Research (http://www.mochida.co.jp/zaidan/), the Senri Life Science Foundation (#S-2144, http://www.senri-life.or.jp/), the Kato Memorial Bioscience Foundation (http://www.katokinen.or.jp/) and the Japan National Society for the Prevention of Blindness (http://www.nichigan.or.jp/link/situmei.jsp). A grant from the National Institute of Health (E13053), was awarded to GA. The funders had no role in study design, data collection and analysis, decision to publish, or preparation of the manuscript.

**Competing Interests:** The authors have declared that no competing interests exist.

* E-mail: furukawa@obi.or.jp (TF); kondomi@med.nagoya-u.ac.jp (MK)

☯ These authors contributed equally to this work.

## Introduction

Paraneoplastic retinopathy (PR) is a progressive retinal disorder caused by an autoimmune mechanism and is associated with the presence of anti-retinal antibodies in the serum generated against neoplasms not associated with the eye [1–4]. The retinopathy can develop either before or after the diagnosis of a neoplasm. Patients with PR can have night blindness, photopsia, ring scotoma, attenuated retinal arteriole, and abnormal electroretinograms (ERGs). The diagnosis of PR is usually made by the identification of neoplasms and anti-retinal autoantibodies in the sera.

PR includes two subgroups: cancer-associated retinopathy (CAR) [5,6] and melanoma-associated retinopathy (MAR) [7–10]. Although CAR and MAR share similar clinical symptoms, the ERG findings

are very different. Both a- and b-waves are severely attenuated in CAR, indicating extensive photoreceptor dysfunction, whereas only the b-wave is severely reduced while the a-wave is normal in MAR, suggesting bipolar cell dysfunction [8,9]. However, it was recently reported that cancers other than melanoma can cause bipolar cell dysfunction [11,12]. Several autoantibodies against retinal antigens have been identified, but a specific antigen associated with bipolar cells has not been identified in patients with CAR and MAR [1–10].

In the current study, we identified autoantibodies against the transient receptor potential cation channel, subfamily M, member 1 (TRPM1) [13–15] in the serum of one patient with lung cancer. The ERG findings in this patient indicated a selective ON-bipolar cell dysfunction. We also investigated the sera of 26 MAR patients and found that two contained autoantibodies against TRPM1. Our results suggest that TRPM1 is one of the retinal autoantigens in at least some patients with CAR or MAR and may cause retinal ON bipolar cell dysfunction.

## Results

### Case report of CAR associated with ON bipolar cell dysfunction

A 69-year-old man visited the Nagoya University Hospital with complaints of blurred vision, photopsia and night blindness in both eyes of three months duration. At this point he was not diagnosed as suffering from any eye disease or systemic disease, including a malignant tumor, and his family history revealed no other members suffering from any eye diseases. On initial examination, his best-corrected visual acuity was 0.9 in the right eye and 0.6 in the left eye. Humphrey static perimetry revealed a severe decrease in sensitivity within the central 30 degrees of the visual field in both eyes (Fig. 1A). Dark-adaptometry of this patient showed a loss of the rod branch. The cone threshold was within normal range. Ophthalmoscopy showed a nearly normal fundus appearance except for slight hypopigmentation at the macula of the left eye, which may be due to age-related changes in the retinal pigment epithelium (Fig. 1B), but fluorescein angiography demonstrated periphlebitis of the retinal vessels (arrows, Fig. 1C). Spectral-domain optical coherence tomography (SD-OCT) showed that the morphology of the retina was normal in both eyes (Fig. 1D).

### Electrophysiological examinations

Recordings of the full-field ERGs from this patient showed that the rod responses were undetectable (Fig. 2). The rod- and cone-mixed maximal response was a negative-type with an a-wave of normal amplitude and a b-wave that was smaller than the a-wave. The a-wave of the cone response had a wide trough, and the b-wave was reduced by 40%. The amplitude of the 30-Hz flicker ERG was reduced by 50%. The photopic long-flash ERG showed severely reduced ON response and normal OFF response. These ERG findings indicated that there was a defect in the signal transmission from photoreceptors to ON bipolar cells both in both rod and cone pathways.

Based on these ophthalmological and electrophysiological tests, we suspected that this patient might have PR and referred him to an internist. The general physical examination including positron emission tomography and computed tomography revealed two abnormal masses in the right lung. Biopsy of these masses confirmed that the masses were small cell carcinomas of the lung.

### Detection of autoantibodies against TRPM1 in the serum of the CAR patient

Based on our ERG examination results, we hypothesized that the serum of this CAR patient may contain autoantibodies against

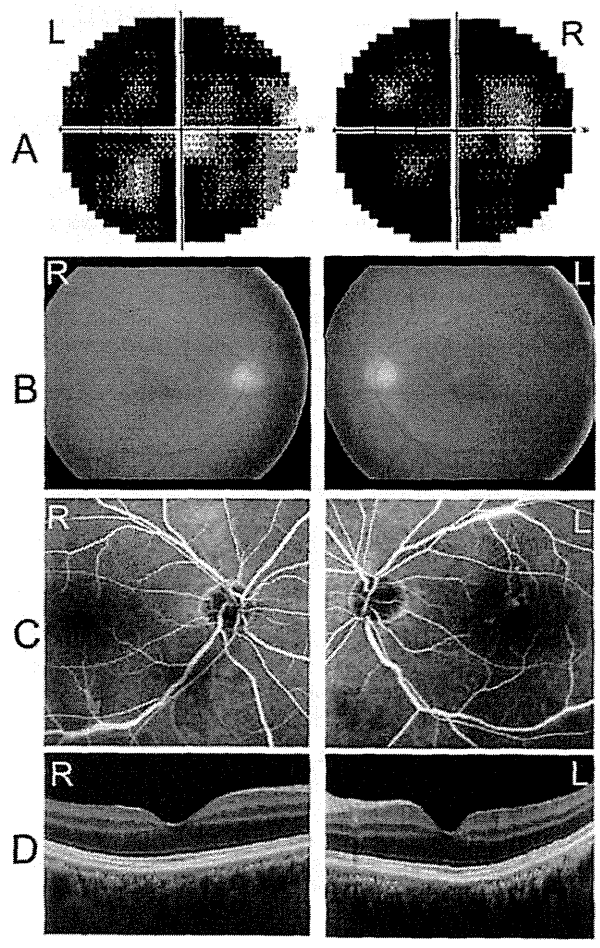


**Figure 1. Ophthalmological findings from a patient with paraneoplastic retinopathy (PR) associated with lung cancer.** (A) Threshold of static visual field (Humphrey, 30-2 program) plotted on a gray scale showing severely decreased sensitivities within the central 30 degrees of the visual field. (B) Fundus photographs of the patient showing a nearly normal fundus. (C) Fluorescein angiograms showing periphlebitis of the retinal vessels (arrows). (D) Spectral-domain optical coherence tomographic (SD-OCT) image of a 9 mm horizontal scan of the retina of our patient. The retinal structure in each retinal layer is normal.
doi:10.1371/journal.pone.0019911.g001

TRPM1. To test this hypothesis, we examined whether or not this CAR patient's serum could recognize human TRPM1 protein by Western blot analysis. We transfected an expression plasmid containing human TRPM1 cDNA with the C-terminal 3xFlag-tag (TRPM1-3xFlag) into HEK293T cells, and carried out a Western blot analysis using whole cell extracts harvested after 48 hrs cell growth. We first confirmed that TRPM1-3xFlag was expressed by cell using Western blot analysis and an anti-Flag antibody. We detected the ~200 kDa TRPM1-3xFlag band in the cell lysates (Fig. 3A).

Next, we performed Western blot analysis on the same lysates using the serum from our CAR patient and a healthy control person. We detected immunostaining of the same size protein, which was confirmed with the anti-Flag antibody, and with CAR serum. The control serum did not present a significant band (Fig. 3B, C). This result showed the presence of autoantibodies against TRPM1 in this CAR patient's serum.